Clim Dyn (2011) 37:253–278
DOI 10.1007/s00382-010-0829-8

A simple hydrologic framework for simulating wetlands in climate and earth system models

Ying Fan · Gonzalo Miguez-Macho

Received: 9 December 2009 / Accepted: 16 April 2010 / Published online: 9 June 2010

Abstract Wetlands are ecosystems of important functions in the earth's climate system. Through relatively high evapotranspiration, they affect surface water and energy exchange with the atmosphere directly influencing the physical climate. Through CH_4, CO_2 and N_2O fluxes, they regulate the biogeochemical cycles, indirectly influencing the physical climate. However, current models do not explicitly include the water table, present under all large and stable wetlands; model wetlands are identified as flat land with wet soil resulting from precipitation events. That is, the wetlands are only 'wetted' from above but not from below by the high water table. Furthermore, without the knowledge of the water table position, estimates of CH_4 and other gases (e.g., CO_2 and N_2O) are poorly constrained. We present a simple hydrologic framework for simulating wetlands based on water table depth. A synthesis of hydrologic controls on wetlands highlights the key role that groundwater plays. It directly feeds wetlands, supports surface-water fed wetlands by maintaining a saturated substrate, and links land drainage to sea level by impeding drainage in lowlands. Forced by routine climate model output (precipitation–evapotranspiration-surface runoff), land topography, and sea level, we simulate the present-day water table in North America at the 1 km scale. We validate the simulation with water table observations and compare regions of shallow water table to mapped wetlands. Our results show that the framework captures the salient features of wetland distribution and extent at regional and continental scales, a direct result of large-scale groundwater convergence that nourishes the lowlands even in arid climates. The low requirement of forcing and computation make the framework easy to adopt in climate and earth system models for simulating wetland responses to climate and sea level change for the present, paleo reconstructions, and future projections.

Keywords Wetlands · Water table · Climate modeling · Earth system modeling · North America

Y. Fan (✉)
Department of Earth and Planetary Sciences,
Rutgers University, New Brunswick, NJ 08854, USA
e-mail: yingfan@rci.rutgers.edu

G. Miguez-Macho
Non-Linear Physics Group, Universidade de Santiago de Compostela, Campus Sur, 15782 Galicia, Spain
e-mail: gonzalo@fmares.usc.es

1 Introduction

Wetlands have important functions in the earth's climate system. Through saturated or near-saturated surface conditions, they supply the atmosphere with potential or near-potential evaporation. Without water shortage, wetland vegetation, through photosynthesis, transpires at near potential rates (Lafleur 2008). The high evapotranspiration (ET) enhances latent versus sensible heat exchange with the atmosphere, shaping boundary layer dynamics and thermal dynamics, directly affecting regional climate. Enhanced precipitation (P) recycling due to widespread wetlands might have helped to sustain the wet conditions in North Africa in mid-Holocene through positive feedbacks (Carrington et al. 2001). Peat accumulation in northern wetlands has been a persistent carbon sink over the Holocene (Smith et al. 2004), and wetlands are thought to be the main natural source of atmospheric methane (CH_4) (Whalen 2005). Thus, via carbon dioxide (CO_2) uptake and CH_4 emission, wetlands participate in the carbon cycle and hence indirectly affect the physical climate through

radiative forcing by the most potent greenhouse gases (water vapor, CO_2 and CH_4).

There is a need to represent wetland dynamics in our climate and earth system models with full carbon cycle feedbacks (Lafleur 2008). However, current models lack a key mechanism that creates and maintains wetlands on the land surface; the land hydrology component of the models does not consider groundwater processes. Without groundwater, wetlands in the models are identified as flat land with wet soil, the latter determined from *P*, ET and surface runoff. That is, wetlands are only 'wetted' from above but not from below by the high water table characteristic of wetland conditions. Furthermore, without the knowledge of water table positions, estimates of CH_4 and other gases (e.g., CO_2 and N_2O) are poorly constrained.

An accurate model simulation of wetlands is also needed to understand wetland responses and feedbacks to the past climate change. Ice-core records reveal marked variations in atmospheric CH_4 at millennium to glacial-interglacial scales which correlate well with the major cooling and warming events (Brook et al. 2000; Loulergue et al. 2008). Changes in CH_4 have been attributed to changes in the extent and location of wetland sources, atmospheric sinks, and marine and permafrost hydrates, but their relative importance remains uncertain (Chappellaz, et al. 1993; Brook et al. 2000; Dallenbach et al. 2000; Kaplan 2002; Valdes et al. 2005; Sowers 2006). Some of the uncertainties stem from the lack of a more precise knowledge on wetland response to changes in global climate and sea level, such as the expansion and contraction of tropical wetlands forced by orbital precession, the initiation and migration of boreal peatlands following the ice sheets, and the shifting of coastal wetlands following sea level change. For example, while the model reconstruction by Kaplan 2002 gave a global wetland area at the last glacial maximum (LGM) greater than under present climate, Valdes et al. 2005 obtained the opposite results.

The lack of explicit wetland mechanisms in the models may have contributed to the uncertainties in paleo reconstructions. Kaplan 2002 identified wetlands as model cells with soil moisture above a threshold and terrain sufficiently flat. While it worked well in humid and flat regions, it missed wetlands in drier climate. In simulating wetland and CH_4 flux to future climate change, Walter et al. 2001a, b constructed a hydrology model that explicitly tracks the position of the water table, a key regulator of CH_4 flux. They found that in order to generate wetlands in arid climate, lateral inflow via rivers-groundwater is needed, for the water table is not only controlled by the vertical *P* and ET flux, but also by the lateral flow among model cells through the rivers and groundwater convergence.

These studies call for a synthesis of the hydrologic mechanisms responsible for wetland conditions, which will lead to the development of a simple method of wetland identification that incorporates the most important of these mechanisms. The objectives of this paper are (1) to attempt a synthesis of hydrologic controls on major wetlands, and (2) to formulate a hydrologic approach for wetland simulation given climate, topography, and sea level, keeping it sufficiently simple to be included in comprehensive earth system models, and to test the approach over the North American continent.

2 Hydrologic controls on wetlands: a synthesis

Figure 1 is a simple conceptual model of hydrologic control on wetlands along a climate and drainage gradient, a hypothetical one for illustrating the end members in a range of climate-drainage combinations. From the left to the right, the climate shifts from a cool-moist alpine regime to a warm-dry coastal setting; the terrain from steep high slopes to flat lowlands; the thin soils over shallow bedrock to thick sandy coastal-plain deposits. Transitions in climate, topography and geology lead to a transition in hydrology: local runoff on the left and regional surface and groundwater convergence on the right. Transitions in hydrology in turn lead to transitions in mechanisms whereby wetlands are formed.

The high, steep terrain on the left, plus the thin soil and low permeability of shallow bedrocks, favors surface runoff and local, shallow subsurface runoff, which combined with low ET can lead to surface ponding and form local wetlands, such as wetland-A in Fig. 1. Located at the high end of the drainage gradient, these wetlands may slowly lose water to the regional water table below, but runoff from episodic rain events or seasonal snowmelt can temporarily out-pace groundwater loss, forming intermittent or seasonal wetlands. Such wetlands are fed by precipitation and local runoff over a small catchment area, and they are 'perched' above the regional water table. As such, they tend to be small in spatial extent, exhibit large temporal variability in water level, and may disappear temporarily or seasonally.

Wetlands on the lowest end of the gradient, such as wetland-D, exist for different reasons. The warm-dry climate results in an atmospheric deficit ($P < \mathrm{ET}$), and the flat terrain over deep soil does not favor local runoff. Despite the lack of local sources, wetlands can form because of remote sources gathered over a large catchment above. The remote source can be river convergence through the river network on land, or groundwater convergence through regional aquifers below, or both. In Fig. 1 plan view, wetland-D, situated along the main stem of a river network, may receive both river and groundwater inflow. River inflow alone is unlikely to

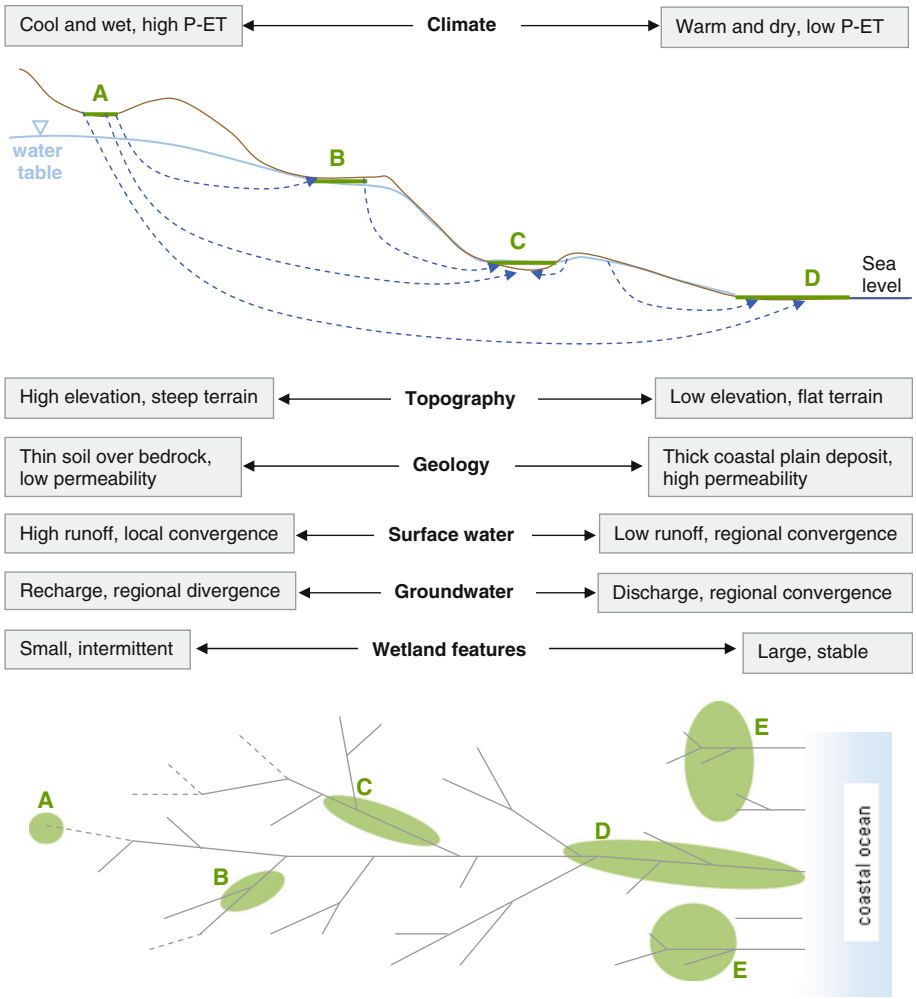

Fig. 1 Schematic hydrologic control on wetlands along a climate and drainage gradient. Wetland-A is fed by precipitation and local surface/subsurface runoff. Wetland D is fed by surface convergence but supported by a shallow water table, and wetland-E is fed by the groundwater, both located in zones of regional groundwater convergence. Wetlands B and C are along a continuum between these end members

sustain a wetland for long periods without the groundwater support from below, which, although may not be a significant input, must maintain a shallow water table to 'hold up' the surface water and prevent leakage loss. Often the surface drainage and shallow groundwater drainage are in the same direction, and where river converges, groundwater is likely to do so as well. Rivers detached from the groundwater may exist for short periods of time along short distances, fed by flash floods from intense rainfall, as observed in a desert where the dry river beds are above the water table and seldom contain water. Thus wetland-D can be fed by both river and groundwater convergence, or primarily by river inflow but supported by groundwater that saturates the land from below. Wetlands-E, however, are away from large river channels and receive groundwater inflow only. Many coastal freshwater wetlands of the world are fed by springs, and they coexist with numerous small streams that derive their source from the same springs. The increased drainage density frequently observed in coastal lowlands is a manifestation of sustained groundwater emergence. As expected, wetlands D and E, at the receiving end of the regional drainage, are likely to be spatially extensive due to a larger catchment area above, and temporally stable due to the longer timescales of regional flow. Temporal stability is most pronounced in wetlands that are mostly fed by groundwater (Hunt et al. 1999; Winter et al. 2001, 2005).

In cold regions of the Northern Hemisphere, frozen soil exerts another control by impeding vertical drainage and limiting lateral drainage to the thin thawed layer seasonally or perennially. As shown in Fig. 2, the depth of frost penetration (bottom of shaded region) increases from a few cm in the mid-latitude to over 1 km in the high arctic, and the depth of seasonal thaw (top of darker gray region) decreases from a complete thaw in the mid-latitude to a few cm in the far north (Nelson and Hinkel 2002), resulting in three soil thermal regimes: never frozen, seasonally frozen, and perennially frozen (permafrost). South of the permafrost limit, drainable soil depth is reduced part of the year, and although groundwater flow can occur under the frost, the latter impedes spring drainage and creates a perched water table at least

part of the year. North of permafrost line, drainable soil depth is reduced all year round, and drainage occurs only part of the year and is confined to the active layer. The impeding effect increases northward due both to the increased spatial extent-depth and the temporal frequency-duration of frost, leading to a northward transition from patchy to continuous wetlands (wetland-F, Fig. 2). Frozen ground is the key factor in the formation of boreal and arctic wetlands, overriding others associated with cold climate such as thin soil (slow weathering) low ET (Woo 2002; MacDonald 2002) and recent glaciation (dense till deposit). This thermal gradient similarly affects high altitudes and contributes to the formation of wetland-A in Fig. 1.

Many wetlands are located somewhere between these end members (Cole et al. 1997; Euliss et al. 2004; Thompson et al. 2007) where both local/vertical and regional/lateral flux contribute to their source, with and without frozen grounds, such as wetlands B and C in Fig. 1. Moving down the drainage gradient, a wetland is in increasingly closer contact with the regional water table, and the relative contribution of local/vertical flux diminishes while that of remote/lateral flux gains significance. Note that the combination of climate and drainage gradients in Fig. 1 is not necessary: wetlands can certainly occur where both climate and drainage are in favor, such as in the humid river valleys and coastal plains of southeastern US (high P + flat lowlands), and the northern peatlands (low ET + flat lowlands + frozen substrate). The conceptual models in Figs. 1 and 2 are helpful for illustrating the end members of climate and drainage conditions that can lead to wetlands, particularly the case that a humid climate is not always necessary provided that there are remote sources by river and groundwater convergence and/or impeded drainage due to frozen grounds.

From a hydrologic perspective, one may characterize the 'wetting mechanisms' as the following: mostly precipitation and local runoff-fed (type-A), mostly surface water-fed but groundwater-supported (type-D), mostly groundwater-fed (type-E), and mostly frozen ground-supported (type-F). The numerous existing classification schemes are based on a combination of physical (flooding regime), geochemical (nutrient dynamics), and biological (flora/fauna) features, and they are designed for mapping and managing wetland resources and understanding community functions (see a succinct summary by Woo 2002). Our goal is not to introduce another classification scheme, but to highlight the key 'wetting mechanisms' that can be readily simulated by current climate and earth system models using routine parameters.

Within this simple hydrologic framework, we now briefly discuss the major wetlands of the world (Fig. 3) with a focus in N. America where our method will be tested with substantial observations. Coastal estuaries and salt marshes are excluded because they are products of tidal dynamics. Some of the discussions below are brief summaries from Mitsch and Gosselink 2007.

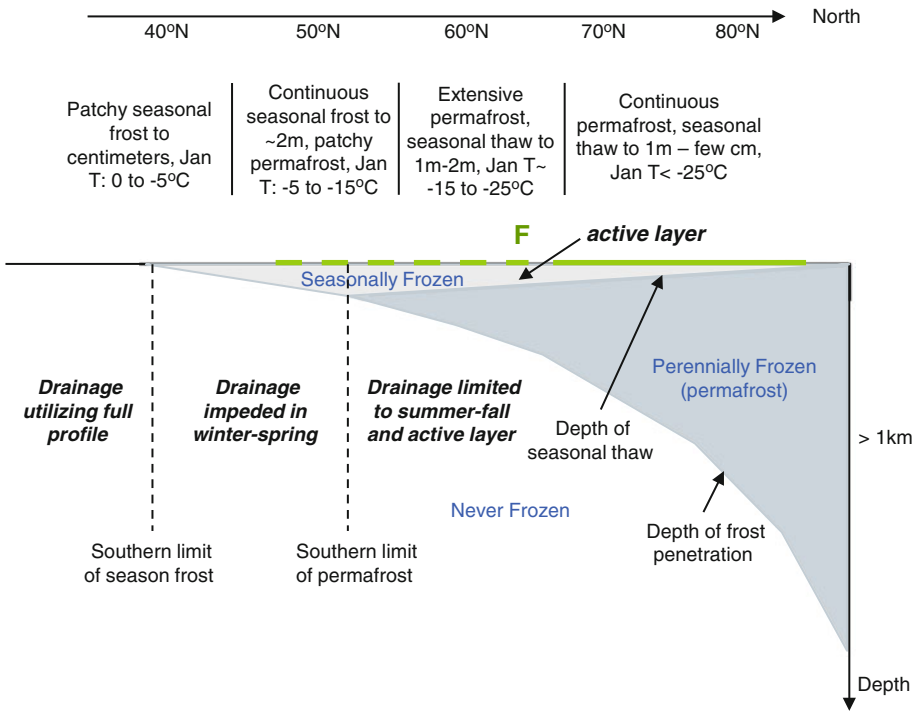

Fig. 2 A schematic of drainable soil depth as affected by the thermal gradient from the mid-latitude to the arctic, the three soil thermal regimes (never frozen, seasonally frozen, and permafrost), the proximate southern limit and the occurrence of wetland F due to impeded drainage

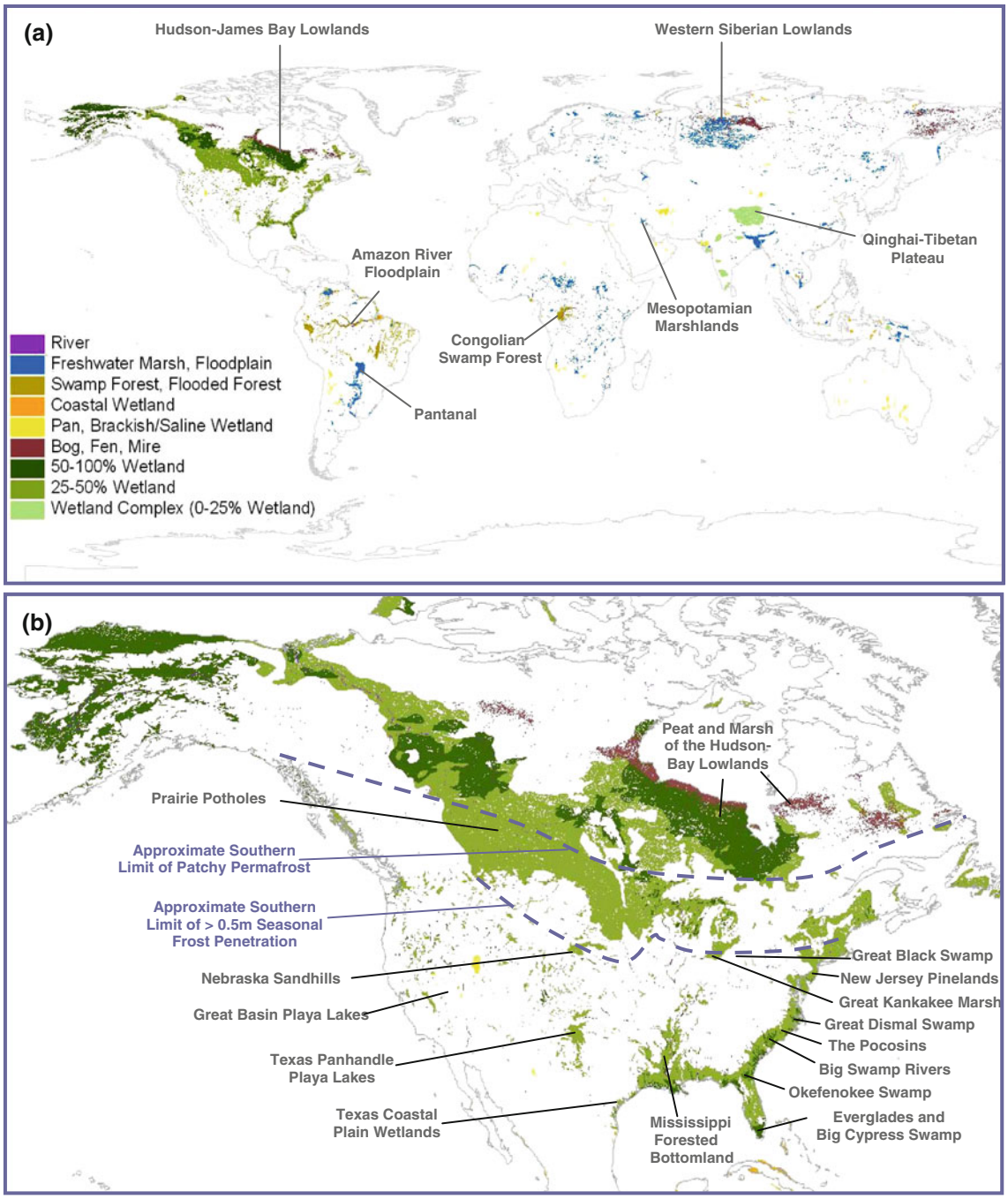

Fig. 3 **a** Modern-day wetland distribution in the world and **b** details over North America, showing the locations of wetlands discussed (from the Global Lakes and Wetlands Database, Lehner and Doll 2004, used with author's permission) and the southern limits where frozen soils influence drainage and wetlands

2.1 Type-A: mostly precipitation and local runoff-fed

These are wetlands formed in local depressions with low-permeability substrate, disconnected from a river network and perched above the regional water table. Examples are the numerous ombrotrophic (rain fed) bogs and poor fens (lacking nutrient-rich groundwater input) found in high altitudes and latitudes all over the world formed in local depressions (e.g., Bosman et al. 1993; Chapman et al. 2003; Hajkova et al. 2006; Thompson et al. 2007; Bastl et al. 2008; Rossell et al. 2009) or breaks in slopes (Winter 1976; Winter et al. 1998). The Prairie Potholes (Fig. 3b) may belong here. From the Dakotas and Minnesota in the US to Manitoba, Saskatchewan and Alberta in Canada, numerous small,

isolated wetlands dot the high plains over glacial tills. The semi-arid climate and low regional relief prevent the development of a dense river network, and the relatively high local relief (hummocks) favors surface and shallow groundwater runoff to local and isolated depressions. Seasonal and sporadic rainfall results in temporally focused water input, and the low-permeability of glacial till prevents rapid leakage, both leading to temporary ponding. ET is the largest sink in the potholes' water budget (Winter and Rosenberry 1995), but groundwater does flow from higher to the lower potholes which rarely go dry (Woo et al. 1993; Rosenberry and Winter 1997; Woo 2002; Winter and LaBaugh 2003). Clearly, the drainage gradient shown in Fig. 1 can occur at multiple scales, and in the potholes region, the relative importance of local versus remote sources can vary.

2.2 Type-D: mostly surface water-fed but groundwater-supported

These are wetlands over saturated grounds with major flow-through rivers, and they occur in several physiographic settings.

2.2.1 Coastal freshwater wetlands

Along the Atlantic and the Gulf coasts of N. America (Fig. 3b), the humid climate feeds many rivers that flow across the broad coastal plains toward the ocean. Along the main stems of the rivers are extensive wetlands, e.g., the Big Swamp Rivers of Georgia and N. Carolina where large forests and marshes are cut through by large rivers and interspersed by small lakes. Other examples are the Everglades and the Big Cypress Swamp, inundated with a shallow surface flow centimeters deep. Such wetlands also develop along the coast of the Great Lakes, e.g., the Great Kankakee Marsh in Indiana-Illinois with rivers meandering through flat lowlands, and the Great Black Swamp in Ohio which was the southern tip of ancient Lake Erie. The Great Lakes wetlands have been mostly destroyed (hence missing in Fig. 3b). Such wetlands are not limited to humid climate; the Mesopotamian Marshlands in Iraq and Iran, at the confluence of Tigris and Euphrates rivers and the home to the Marsh Arabs for 5,000 years, is located in a desert (Fig. 3a).

2.2.2 Tropical-subtropical forests

Large forested wetlands exist along major rivers in the tropics and subtropics. Forested floodplain covers up to 25% of Amazon basin in S. America, with flood level reaching 10 m during flood season. The Congolian Swamp Forest is formed in a depression in the mid-reach Congo River in equatorial Africa, with 1 m of standing water in the rainy reason. The extensive bottom-land hardwood forest in the lower Mississippi valley, which has been largely destroyed since settlement, is another example of flooded forests over saturated lowlands.

2.2.3 Inland floodplains

The Pantanal in S. America is situated in a large tectonic depression under the upper Paraguay River and flooded annually. Flooding from March to May supports lush aquatic vegetation, and in the dry season the landscape reverts to a savanna. River flooding maintains the wetlands and groundwater plays a passive role in this regard (Girard et al. 2003). But the numerous lakes and wetlands that dot the Pantanal in the dry season indicates a shallow water table (Barbiero et al. 2002).

2.3 Type-E: mostly groundwater-fed

These wetlands are 'wetted from below' by groundwater upwelling, and they often coexist with headwater streams that derive their source from the same springs.

2.3.1 Coastal freshwater wetlands

Along the Atlantic coast, large wetlands are found over the flat and sandy coastal-plains. Examples are the maple-white cedar swamps of the Pinelands of New Jersey (Mandernack et al. 2000), the Great Dismal Swamp (bold cypress) of Virginia and N. Carolina, the Pocosins (evergreen shrub bogs) of the Carolinas, and the Okefenokee Swamp in Georgia and Florida which feed the headwaters of two river systems: the Suwannee River, flowing southwest through Florida to the Gulf of Mexico, and the St. Mary's River, flowing southward and then eastward to the Atlantic Ocean.

2.3.2 Inland freshwater wetlands in semi-arid climate

The Nebraska Sandhills is a region of stabilized sand dunes with interdunal valleys that contain numerous shallow lakes and wetlands despite the low P over the region (Winter 1986). The dune field is part of the Ogallala formation, a large sandy aquifer that extends throughout the central Great Plains of the US and is recharged in the Rockies to the west (Gutentag et al. 1984). The high permeability of the sandy substrate and the stable water level suggest that the wetlands are directly connected to this vast groundwater reservoir (Gosselin et al. 1999; Winter et al. 2001).

2.3.3 Internal drainage basins

The arid, internal drainage basins of the world contain numerous freshwater, brackish and saline wetlands. In the

Great Basin of the western US, large snowfall in the high mountains feeds the springs that emerge at the foothills, as well as streams that empty into the alluvial fans, filling the valley aquifers and raising the water table to the surface in the flat valleys (Snyder 1962; Fan et al. 1997; Patten et al. 2008). The high ET in the valleys is the only water outlet, leaving salt behind and forming saline lakes and playas that support salt-tolerant vegetation. The name of the city Las Vegas in the arid Nevada implies a swampy condition. Another example is the Texas Panhandle playa wetland system which includes 19,000 playa lakes (http://www.texasep.org/cpft/php.html). Brackish and saline lakes and mud flats also dot the Qinghai-Tibetan Plateau, a vast interior drainage in central Asia. In the arid East Africa Rift Valley, numerous freshwater swamps and blister wetlands are fed by groundwater convergence and springs issued along fault lines (Owen et al. 2004; Ashley et al. 2002).

2.4 Type-F: mostly frozen ground-supported

These wetlands, fed by precipitation/snowmelt and surface/subsurface runoff, exist largely because of the frozen soil in the shallow depths which prevents drainage. The southern limits of significant seasonal frost penetration (>0.5 m) and patchy permafrost are shown in Fig. 3b, defining regions where frozen ground contributes to wetland formation.

2.4.1 Subarctic marshes, bogs and fens

Vast wetlands develop in the boreal and subarctic lowlands of N. America and Eurasia due to cold climate and poor drainage. Although P is low, ET is even lower, giving a net atmospheric surplus. But most significantly, frozen ground only thaws to a shallow depth, restricting vertical drainage and creating a perched water table (Woo 2002; Price et al. 2005). An example is the Hudson Bay Lowlands in Canada: an extensive wetland complex of marshes, peatlands and forested or open bogs and fens (MacDonald 2002), and in western Siberia: a vast lowland region that is home to extensive peatlands, shallow lakes and river floodplains.

3 The importance of groundwater and the deficiency in current models

Groundwater-wetland interaction can be complex at local and weather-event scales (Rosenberry and Winter 1997), but the following broad patterns seem to emerge at continental and climate scales. First, groundwater can be the main source for wetlands where local source is limited but regional groundwater convergence is significant. Regional groundwater flow is the dominant drainage in arid climate and/or with efficient aquifers where the water table drops below local relief and discharge occurs at regional depressions farther down, feeding rivers, oases and wetlands far away from its recharge source (Schaller and Fan 2009). In this way, groundwater gathers the low P over a large area and concentrates it over a small discharge zone. The freshwater wetlands near Chilean coast, in the Atacama Desert, own their persistence to regional groundwater convergence from the high Andes (Squeo et al. 2006).

Second, groundwater is directly below and supports extensive wetlands primarily fed by surface water through river flooding. But without saturated substrates, surface water fed wetlands cannot persist in dry places or seasons. Raid and Wood 1976 has long recognized the role of the groundwater in sustaining floodplain wetlands, often thought as surface water features. They stated that, "Often the floodplain may take the form of a very level plane occupied by the present stream channel, and it may never, or only occasionally, be flooded…. It is this subsurface water that controls to a great extent the level of lake surfaces, the flow of the streams, and the extent of swamps and marshes". Influenced by Raid and Wood 1976, the National Wetland Inventory by the US Fish and Wildlife Service (USFWS) classifies floodplain wetlands as Palustrine, not Riverine (i.e., not associated with rivers) (Cowardin et al. 1979).

Third, groundwater is the link between land drainage and the sea level. Except for low desert valleys of internal drainage, the water table cannot drop below the sea level, and hence it is found close to land surface in coastal regions. This is the real reason that large, permanent wetlands are found at coastal lowlands, such as along the Atlantic and Gulf coast in the US. Lacking the water table, current models allow drainage to occur below sea level in flat coastal regions, thus unable to produce the wetland conditions found in nature (Miguez-Macho et al. 2008). This land drainage-sea level link was evident over the past when global sea level fell/rose over 120 m over glacial-interglacial cycles. As the sea level fell, vast continental shelf was exposed, and in response to the lowered baseline, coastal groundwater discharge increased and freshwater springs appeared in the newly emerged shelves, forming 'coastal oases' and moving inland ecosystems seaward (Faure et al. 2002). As sea level rose in late Pleistocene to early Holocene, land drainage backed up and water table rose. The attenuation of sea level rise in mid-Holocene led to a period of relative stability when many of the modern-day coastal wetlands stabilized, e.g., on the Atlantic coastal plains in southeastern US (Gaiser et al. 2001), in southern England (Waller et al. 1999), on the Galician coast in northwestern Spain (Bao et al. 2007), along the Adriatic coast in southern Italy (Boenzi et al. 2006), and at the coastal swamps of Trinidad (Ramcharan 2004). The sequence of peat deposits in coastal sediments in the

Venetian plain in northeastern Italy are linked to wetland formation and burial due to millennium-scale sea level change (Miola et al. 2006). The sequence of wetland flora preserved in volcanic deposit in northern New Zealand are linked to changes in groundwater condition as sea level fluctuated across the coastal plain (Marra et al. 2006). Thus at millennium to glacial-interglacial time scales, coastal wetlands are dynamically linked to sea level change, facilitated by the coastal water table forever adjusting to the sea level.

Fourth, the water table depth is a key control of wetland functioning (Lafleur 2008). It influences wetland productivity and species diversity (Grevilliot et al. 1998; Hayashi and Rosenberry 2002; Groom 2004; Dwire et al. 2006; Stromberg et al. 2007), and it is a regulator of CO_2, N_2O, and particularly CH_4 fluxes from wetlands (Moore and Knowles 1989; Davidson et al. 2000; Jungkunst and Fiedler 2007; Jungkunst et al. 2008). At the ecosystem level, net CH_4 flux from a given wetland is the balance between production by methanogenic bacteria in the anoxic zone below the water table, and oxidation by methanotrophic bacteria in the oxic zone above the water table (Whalen 2005). Other factors equal, a shallow water table allows more CH_4 to survive the upward diffusion (Moore 1994; Funk et al. 1994). A rapidly falling water table may cause quick release of CH_4 bubbles by ebullition (Moore et al. 1990; Windsor et al. 1992). A seasonal reduction in water table depth transformed a temporal swamp from a CH_4 source to a sink (Harris et al. 1982). Such process and ecosystem-level understanding has led to quantitative models of wetland CH_4 flux (e.g., Walter and Heimann 2000). In applying these models, the spatial extent of wetlands and the water table depth, both sensitive to climate, are essential pieces of information as model input (Ju et al. 2006; Dunn et al. 2007). However, the water table position is not yet established at continental to global scales due to a lack of observations and explicit representation in current models. This makes it difficult to construct the large-scale water table dynamics, and without it, applications of process-based CH_4 models are poorly supported.

The apparent importance of water table in wetland formation, wetland response to sea level change, and wetland CH_4 flux may be a sufficient justification for a hydrologic framework of wetland delineation that takes into account the water table. But the groundwater is not routinely considered in current models and the approaches in simulating wetlands (e.g., Kaplan 2002; Valdes et al. 2005; Decharme et al. 2008), nor is cell to cell groundwater flow (e.g., Merot et al. 2003; Gedney and Cox 2004) important to sustaining wetlands in arid climate relying on remote sources and coastal regions constrained by the sea level. Several studies applied the TOPMODEL (Beven and Kirkby 1979) concept to characterizing water table distribution within a model grid (e.g., Koster et al. 2000; Ducharne et al. 2000; Walko et al. 2000; Chen and Kumar 2001; Seuffert et al. 2002; Gedney and Cox 2003; Yang and Niu 2003), which allows local topography to redistribute soil water, based on the fact that TOPMODEL is a powerful tool for characterizing hillslope to catchment scale hydrologic equilibrium in a humid climate and with sufficient topographic relief. However, at larger scales where climatic and geologic variabilities emerge, and in a dry climate where the water table falls below the local valleys, the advantage of TOPMODEL is less clear. In addition, without model cell to cell flow, the local water table has no communication to remote recharge or discharge zones and to the sea level. We wish to emphasize that the water table is not just a local identity, but also a trans-continental surface tied to the sea level (Schaller and Fan 2009). It is the lateral divergence/convergence at the inter-cell scales that are lacking in current approaches and need to be considered in wetland simulations (Kaplan 2002; Walter et al. 2001a, b).

While recent effort begins to explicitly include groundwater in regional climate models, this is not yet operational in global climate and ecosystem models participating in the full carbon cycle research. Thus a simple mechanistic framework would be useful for translating standard climate model output into water table conditions so that wetlands can be inferred. That is, we seek a framework that translates current model simulations of land surface fluxes (P, ET, surface runoff), as is, without the groundwater, into water table conditions given the topography and sea level, in an 'off-line' mode. This framework is the main motivation for this study. We define this framework as satisfying the following. First, it must link the water table conditions to the climate, terrain, and sea level, fundamental drivers of land hydrology. Second, it must incorporate the most important 'wetting mechanisms' which, as emerged from the synthesis above, point to the role of the groundwater in supporting the large and stable wetlands of the world. Third, it must explicitly calculate the water table depth for biogeochemical flux estimates. And fourth, it must remain sufficiently simple to be attached onto comprehensive earth system models using routine model output.

In this report, we test the utility of the water table depth as an indicator of large and stable wetlands. The climatologic mean water table depth reflects the long-term water balance under a given climate. Its height is adjusted to balance inflow and outflow, and hence it communicates vertically with the climate (P–ET) and laterally with the neighbors, through groundwater divergence/convergence, and ultimately with the sea level. As such, it integrates the effect of climate and the terrain locally and remotely (up and down the drainage gradient) and globally (the sea level). It reflects the long-term climate condition rather

than weather events and is directly responsible for prolonged and stable wet conditions for peat accumulation and vegetation successions. Thus the climatologic mean water table may serve as a first-order indicator of the wetness of the land. In the following, we simulate the modern-day equilibrium water table and compare it with mapped natural wetlands in North America where observations in both water table depth and wetland area are most abundant. The continent also hosts a wide range of wetlands from the arctic tundra to the sub-tropical lowlands, providing a good test bed for the proposed framework.

4 Hydrologic equilibrium and the water table depth

Assuming that the modern-day land hydrology is in equilibrium with the climate and the sea level (Marshall and Clarke 1999) we model the position of the water table resulting from the long-term balance between the vertical, climate-induced flux across the water table (recharge R, Fig. 4a) and the lateral, geology-topography-induced flow below and parallel to the water table (drainage, Q), the latter constrained by the sea level (head boundary condition). The result is a smooth, undulating surface that begins at the sea level surrounding a continent and extends into the continent beneath the land topography, occasionally appearing at the land surface as wetlands, rivers and lakes through upward seepage (Qr, Fig. 4a). Over a hillslope cell (size Δx by Δy), recharge (R) balances lateral divergence (Q) to the lower neighbors:

$$R\Delta x\Delta y = \sum Q \tag{1}$$

In a valley cell, lateral convergence (Q) balances upwelling into rivers-wetlands (Q_r):

$$\sum Q = Q_r \tag{2}$$

Equ.2 also applies to a coastal cell where groundwater must emerge before the sea (Q_r).

4.1 Groundwater flow equations

The lateral groundwater flow between model cells (Q) is calculated using Darcy's Law and the Dupuit-Forchheimer Approximation (2D flow) (see, e.g., Freeze and Cherry 1979), which relates the slope of the water table to the flow rate:

$$Q = wT\left(\frac{h - h_n}{l}\right) \tag{3}$$

where Q is the flow between the center cell and its neighbor n, w is the width of the interface between the cells, T is the transmissivity between the cells, h is the water table head in the center cell referenced to the sea level, h_n is the water table head in neighbor n, and l is the distance between the

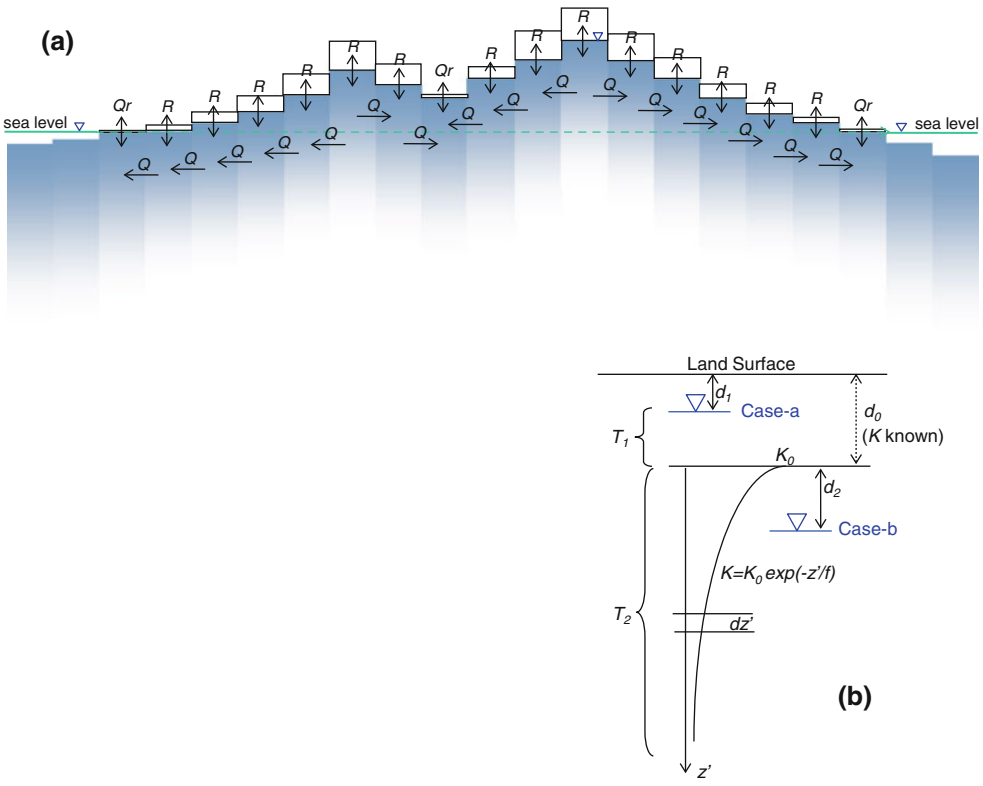

Fig. 4 **a** Schematic of the 2D groundwater model to simulate the climate (recharge R), terrain (lateral flow Q) and sea level (boundary condition) control on water table depth over a continent. In upland cells, recharge balances lateral groundwater divergence to lower neighbors. In valley or coastal cells, lateral groundwater convergence discharges into wetlands and rivers, **b** details of calculating flow transmissivity, T, for Case-a, water table within the depth of known soil hydraulic conductivity (K), and Case-b, water table below the known depth where K is assumed to decrease exponentially with depth

two. To obtain flow transmissivity, T (product of hydraulic conductivity and the flow cross section height), we examine two cases (Fig. 4b): the water table above or below the depth (d_0) with known soil hydraulic conductivity, $K = K_0$. The distinction is necessary because global soil datasets do not include information below the top $\sim$2 m of land surface. In Case-a, the water table is above the depth with known K and the transmissivity is,

$$T = T_1 + T_2 \tag{4a}$$

$$T_1 = K_0(d_0 - d_1) \tag{4b}$$

$$T_2 = \int_0^\infty K dz' = \int_0^\infty K_0 \exp\left(-\frac{z'}{f}\right) dz' = K_0 f \tag{4c}$$

where d_1 and z' are defined in Fig. 4b, and K decreases exponentially with depth from the known value of K_0,

$$K = K_0 exp(-z'/f) \tag{5}$$

where f is the e-folding depth (discussed below). In Case-b, the water table is d_2 below the known K,

$$T = \int_{d_2}^\infty K dz' = \int_{d_2}^\infty K_0 \exp\left(-\frac{z'}{f}\right) dz' = K_0 f \exp\left(-\frac{z - h - d_0}{f}\right) \tag{6}$$

where z is land surface elevation of the center cell.

4.2 Topography and soil

Digital land elevation is obtained from the US Geological Survey (USGS) GTOPO30 product at the 30 sec. resolution (<1 km) (http://eros.usgs.gov/#/Find_Data/Products_and_Data_Available/GTOPO30). Simulation is performed at 30 sec. grid size to balance the need to resolve kilometer-scale wetlands, to compare with water table observations (made at point scales), to keep computation and data storage feasible for global simulations, and to ensure that the data used here has global coverage. Land elevation and slope are shown in Fig. 5a, b which reveal low and flat areas prone to poor drainage and/or groundwater convergence, terrain conditions favorable for wetland formation.

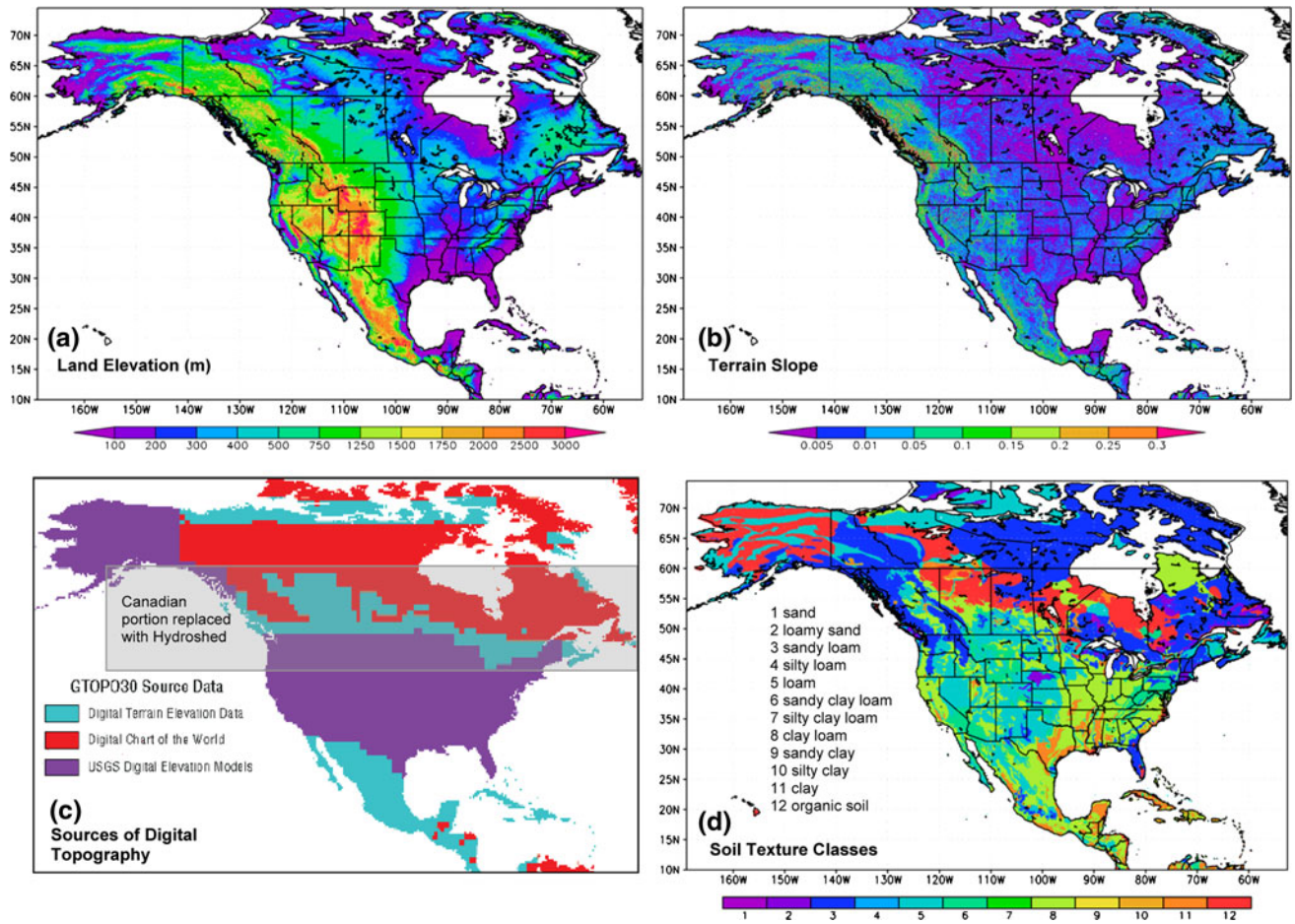

Fig. 5 **a** Land elevation, **b** slope, **c** sources of GTOPO30 product (http://www1.gsi.go.jp/geowww/globalmap-gsi/gtopo30/gifs/gt30src.gif) with southern Canada replaced with USGS Hydroshed, and **d** soil textural classes used in the simulation

We note that GTOPO30 is derived from several sources with varying horizontal spacing and vertical accuracy (http://www1.gsi.go.jp/geowww/globalmap-gsi/gtopo30/gifs/gt30src.gif). The boundaries in Canada (Fig. 5c, between blue and red) show up prominently in the calculated local slope because the red region is 2–4 times coarser than the blue region. These artificial boundaries in slope remained in the simulated water table (Fan et al. 2007; Miguez-Macho et al. 2008) which is significantly shallower in the region of coarse terrain resolution. Because the interest here includes Canada, we improve the data by replacing GTOPO30 with the USGS Hydroshed product (http://hydrosheds.cr.usgs.gov/) where it is available (gray shade, Fig. 5c). Hydroshed is based on shuttle radar measurements over the world (uniform source), at the 3 sec. grid resolution (averaged to 30 sec. here) and referenced to the same geodesic coordinates as GTOPO30. However, it only covers the south of the 60°N parallel. Therefore the artificial boundaries in the north, along the 60°N, 67°N, and 70°N parallels, remain in the slope (Fig. 5b). This is unfortunate because terrain slope is a key control on drainage, and its patchwork nature remains in the simulated water table depth. However, with the ever improving coverage and quality of global digital terrain data, this issue will cease to exist in the future.

Soil information is derived from UNESCO Food and Agriculture Organization (FAO) digital soil map of the world at the 1° spacing (http://www.ngdc.noaa.gov/ecosys/cdroms/reynolds/reynolds/reynolds.htm). Fractions of silt, clay, sand, and organic carbon are used to produce 12 soil-texture classes defined by the US Department of Agriculture (http://soils.usda.gov/education/resources/lessons/texture/). Organic soil (peat) is identified as organic carbon >12% (e.g., Brandy 1984). The 12 soil classes (Fig. 5d) are assigned hydraulic parameters based on empirical relationships (Clapp and Hornberger 1978) widely used by the climate and hydrologic modeling communities.

4.3 Hydraulic conductivity

To calculate groundwater flow, the hydraulic conductivity K for the geologic material must be known at depth, but global soil datasets do not go beyond the top 2–3 m of land surface. Lacking actual measurements, we adopt common assumptions on the vertical distribution of permeability. Porosity and permeability of earth materials generally decrease with depth because pressure-heat release and weathering processes initiate at the surface. Over kilometers, the decrease appears linear in competent rocks like sandstone and exponential in less competent rocks like shale and mudstone (Deming 2002). At the scales of tens of meters, such trends are less obvious. In watershed modeling it is widely assumed that the decrease is exponential with depth (e.g., Beven and Kirkby 1979), in the form of Equ.5, which we adopt for this study.

The value of f in Equ.5, reflecting sediment-bedrock profile at a location, depends on the balance among tectonics, in situ weathering, and erosion–deposition. It is a complex function of climate, geology and biota. But the balance depends strongly on terrain slope (e.g., Ahnert 1970; Summerfield and Hulton 1994; Hooke 2000); the steeper the terrain, the thinner the regolith. Climate also plays an important role, but the mechanisms are more complex (Walling and Webb 1983; Hooke 2000) e.g., low rainfall produces low sediment runoff, leading to sediment accumulation and deep regolith; high rainfall leads to deeper percolation and denser biota, both enhancing in situ weathering and leading to deeper regolith as well (e.g., Langbein and Schumm 1958; Dendy and Bolton 1976). For simplicity with only the first order control, we consider the terrain slope only, in determining f.

The functional relationship between f and terrain slope s is determined by calibration to best reproduce water table observations. Through our earlier work in temperate N. America (Fan et al. 2007; Miguez-Macho et al. 2008), we obtained the following hyperbolic function of f with terrain slope s:

$$f = \frac{100}{1 + 150s}, \quad f > 2.5\,\mathrm{m} \tag{7}$$

The map of f is shown in Fig. 6a, with deep soil (large f) associated with flat terrain and shallow soil with steep slopes. While this function worked well in the temperate regions, our earlier experiments show that it leads to a consistent low bias in the simulated water table head in cold climate with frozen soil. The latter is hydrologically manifested as impeded drainage similar to a thin soil mantle overlying bedrocks or other low-permeability substrates. We modify Equ.7 to include the temperature control on drainage depth. It appears that both the seasonal frost depth and the permafrost thaw depth roughly follow the spatial pattern in winter air temperature (Fig. 6b) (see a synthesis by Nelson and Hinkel 2002). Soil thermal properties (e.g., presence of peat), geothermal gradient, snow depth and soil water content also influence the freeze–thaw depth. But we maintain simplicity and consider only the first-order control by introducing a two-piece linear temperature modifier, fT,

$$fT = 1.5 + 0.1T \ (-14^{\circ}\mathrm{C} < T < -5^{\circ}\mathrm{C}, fT \le 1) \tag{8a}$$

$$fT = 0.17 + 0.005T \ (T < -14^{\circ}\mathrm{C}, fT \ge 0.05) \tag{8b}$$

where T is January mean surface air temperature in °C (Fig. 6b). Equation 8a, 8b is plotted in Fig. 7 (inset), where −5°C corresponds to the approximate southern limit of significant seasonal frost penetration (>0.5 m) (US Department of Agriculture 1941), and −14°C corresponds to the

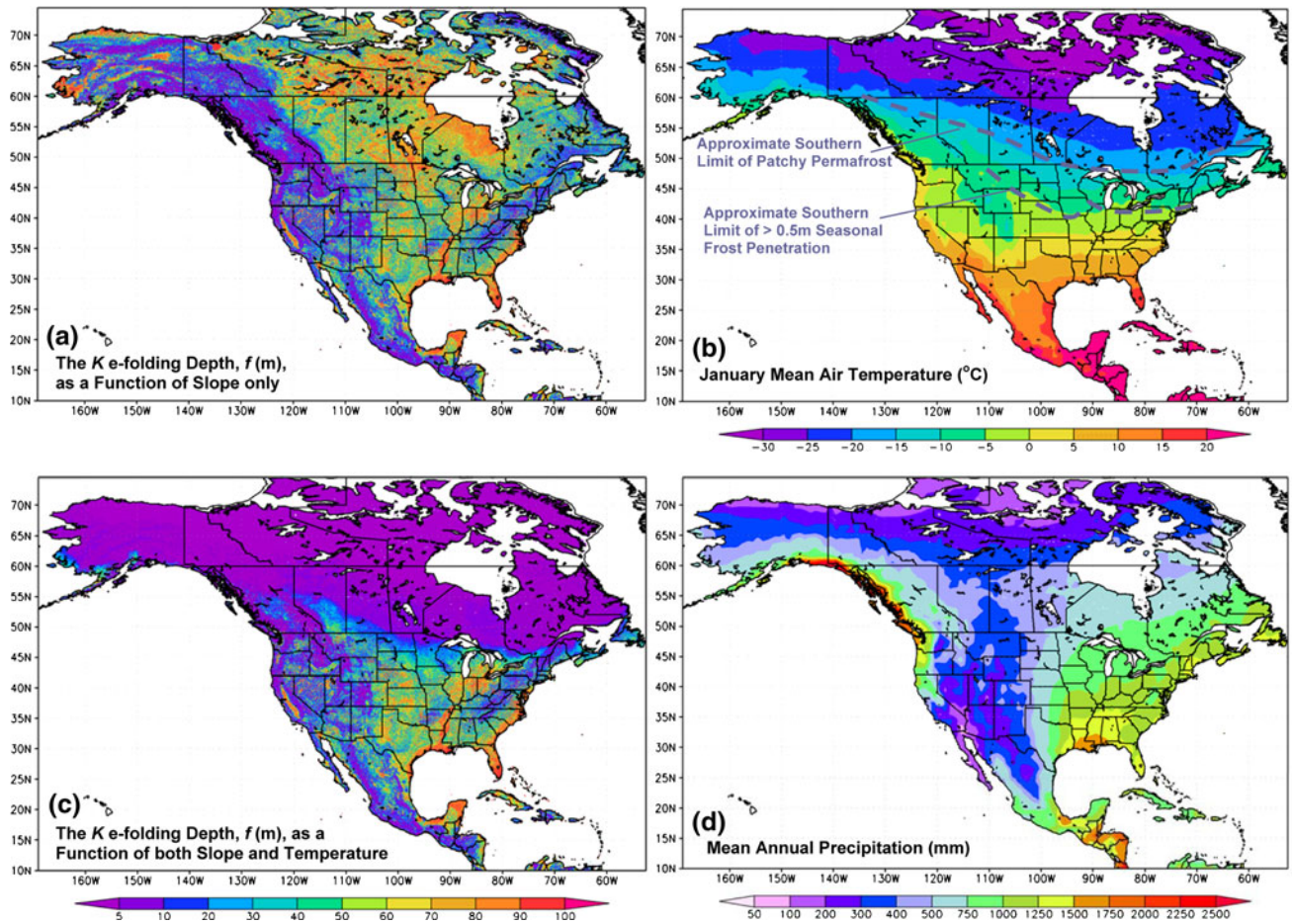

Fig. 6 Parameterizing the hydraulic conductivity (K): **a** the e-folding depth (f) as a function of terrain slope only, **b** January mean surface air temperature used to determine the effect of frozen ground on f, and **c** modified f, as a function of both terrain slope and January temperature. Mean annual precipitation (mm) is shown in (**d**) to aid discussions in the text

approximate southern limit of patchy permafrost associated with peat deposits (Nelson and Hinkel 2002). The slopes of the lines are adjusted to best reproduce observed wetland areas in these two thermal regimes. The final f value is the product of Equ. 7 and 8a, 8b, plotted in Fig. 7 as a function of terrain slope at different January temperatures. The result is a diminishing soil depth (lower f) at steeper slopes and lower temperature. As shown in the map of Fig. 6c, the final f reflects terrain slope in the south but winter temperature in the north. Soil is generally shallow where the land is steep and/or the climate is cold as in high altitudes and latitudes, and it is generally deep where the land is flat and the climate is warm as in the large alluvial valleys and coastal plains in southeast US and the internal drainage basins in the western US.

Lateral hydraulic conductivity is needed to calculate cell to cell flow, but global soil datasets only provide vertical conductivity. Lacking observations, we rely on the concept

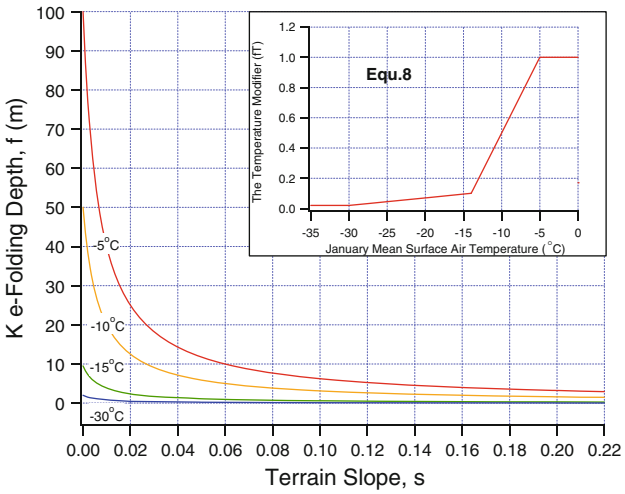

Fig. 7 The temperature modifier (inset) and the dependence of f (K e-folding depth) on terrain slope at different January temperatures

Table 1 Vertical hydraulic conductivity and anisotropy ratio used in calculating lateral groundwater flow

Soil texture class		Vertical K (m/day)	Anisotropy ratio
No.	Name		
1	Sand	15.206	2
2	Loamy Sand	13.504	3
3	Sandy Loam	2.998	4
4	Silt Loam	0.622	10
5	Loam	0.605	12
6	Sandy Clay Loam	0.544	14
7	Silty Clay Loam	0.121	20
8	Clay Loam	0.216	24
9	Sandy Clay	0.190	28
10	Silty Clay	0.086	40
11	Clay	0.112	48
12	Peat	0.691	2

of anisotropy, relating the lateral conductivity, K_L, to the vertical, K_V, through the anisotropy ratio, $\alpha = K_L/K_V$. It is well known that soils and rocks of sedimentary origin exhibit stratified structure, leading to significant anisotropy, with α ranging 1–1000 (e.g., Freeze and Cherry 1979). We apply a crude rule based on the clay content of the soil, for clay has a strong effect on anisotropy due to its platy mineral form and its low permeability as a sedimentary unit. The set of values we chose (Table 1) are well within the range observed in nature.

4.4 Water table recharge

Recharge (R in Equ.1 and Fig. 4), or the net flux across the water table as defined in Fan et al. 2007, is difficult to quantify without coupled soil moisture and water table monitoring or coupled model simulations, because this flux depends on the state of both the soil and groundwater reservoirs. Field observations invoke mass balance over a plot or a small catchment by observing other hydrologic components and inferring recharge, by tracer studies, and by stream flow separation into quick and slow (base-flow) components, the latter sustained by groundwater from recharge. These methods rely on varying assumptions, depend on the periods and scales of studies, and are limited to local estimates. A global field of climatologic flux across the water table can only be achieved by representing the coupled soil moisture and groundwater dynamics in climate models. As mentioned earlier, this is not yet feasible, and some form of surrogate is required.

In this study, we use the observation-based annual rainfall (P) over 1979–2007 minus ET and surface runoff (Q_s): $R = P - \mathrm{ET} - Q_s$, the latter two from simulations by three land hydrology models in the Global Land Data Assimilation System (GLDAS) (Rodell et al. 2004). That is, what does not evaporate-transpire or run off to local streams will enter the groundwater reservoir as water table recharge. Because these models do not include the water table and groundwater flow, the latter have no feedbacks to this flux. But at the present such water balance-based recharge is the closest to a globally consistent estimate at climatologic time scales. It is routinely available from climate model simulations, paleoclimate model reconstructions, and future climate change scenarios, making the method useful for such applications.

The three land models used are CLM (10 soil layers to 3.44 m depth), Mosaic (three layers to 3.50 m), and Noah (four layers to 2.0 m) (http://disc.sci.gsfc.nasa.gov/services/grads-gds/). GLDAS models simulate land surface fluxes that assimilate surface observations (satellite vegetation leaf area index and land surface skin temperature), driven by observation-based atmospheric fields (Rodell et al. 2004). They also characterize sub-grid variability essential to land hydrology. Being such, the simulated hydrologic fluxes contain lower atmospheric bias compared to using climate models. As shown in Fig. 7, the three recharge estimates are similar in spatial patterns but different in magnitudes, due to differences in model soil configuration and flux parameterization, despite identical atmospheric forcing (e.g., identical P, Fig. 6d). The large difference among the three reflects the uncertainty in recharge estimates. To evaluate sensitivity of the simulated wetlands to recharge forcing, we apply all three estimates in this study.

Some areas receive zero recharge in Mosaic and Noah estimates (Fig. 8b, c). While this occurs naturally in river valleys and coastal zones where convergent groundwater discharges to rivers and wetlands, it cannot be so in high altitudes such as in the Colorado Rockies. Recharge from snowmelt feeds mountain streams which flow all year around. A zero recharge is inconsistent with this observation. It is also inconsistent with the concept of climatologic equilibrium water table. Without recharge and with lateral divergence as in the Rockies, the water table will drop indefinitely, until valley recharge backflows to the mountains which is clearly unlikely. Lacking better alternatives, we set a minimum recharge as 10 mm/year mainly for the sake of numerical stability.

Conversely, the recharge in the valleys is unrealistically high, particularly in the desert closed basins of the western US. For example, Noah recharge in the Great Salt Lake Valley of Utah is higher than the surrounding mountains (Fig. 8c), inconsistent with the understanding of closed basin hydrology that valley evaporation is the only water outlet from the system (Snyder 1962; Lines 1979; Bowler

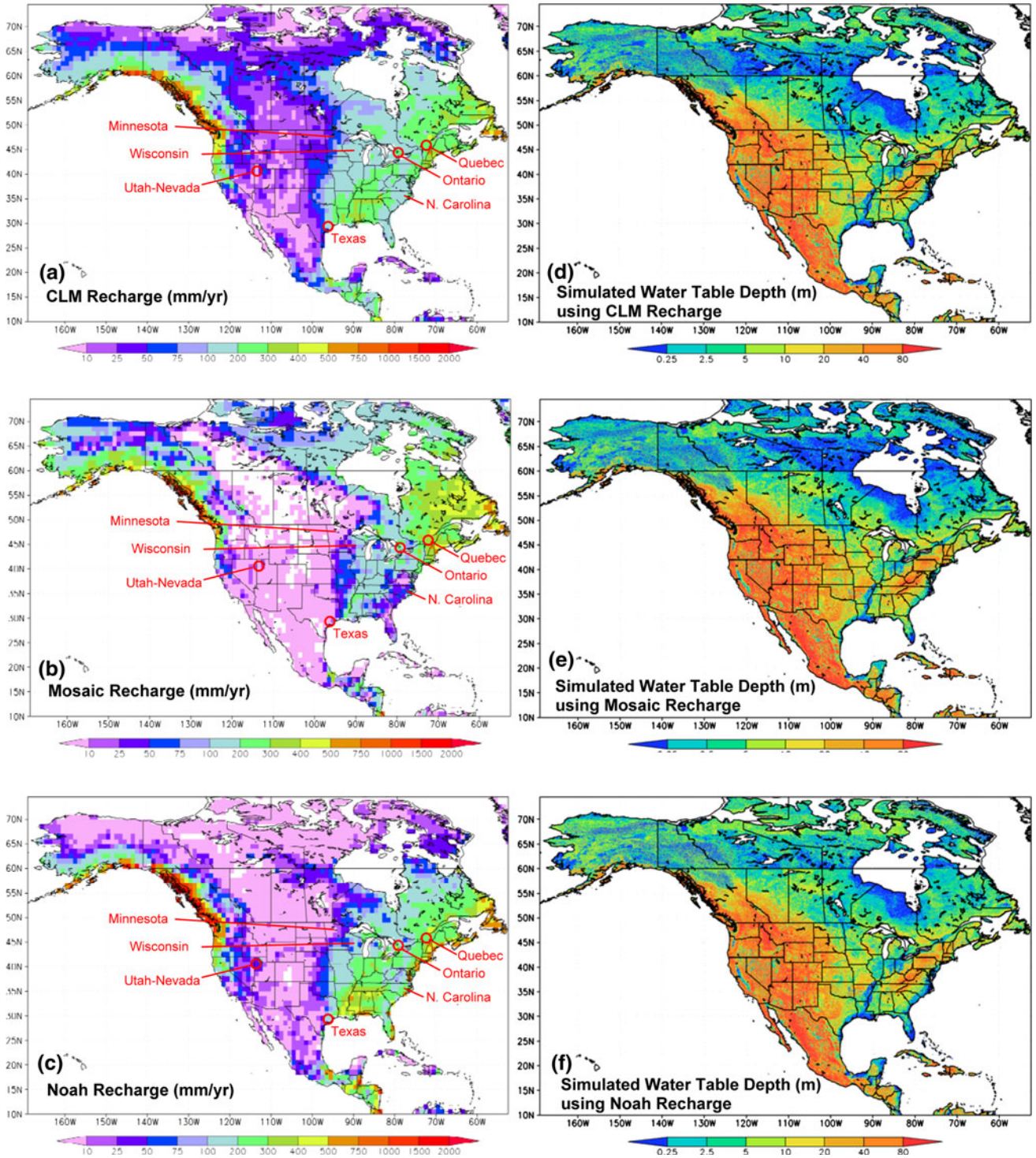

Fig. 8 *Left* column, annual recharge (mm) from three land hydrology models (CLM, Mosaic, and Noah) showing locations where comparison with observations are made (discussed later). *Right* column: simulated equilibrium water table depth (m) using the three recharge estimates

1986; Duffy and Al-Hassan 1988; Fan et al. 1997). Recharge in these valleys must be negative, balancing the high snowfall in the mountains that flow into the valleys. Without this outlet, the modeled water table will be biased high. However, it is difficult to set a cap in all valleys across the continent. This issue is left unaddressed and needs to be considered in the validation and wetland comparison later.

4.5 Boundary conditions and the simulations

The simulation is performed at a grid resolution of 30 sec., or ~912 m × 927 m at 10°N (southern end of domain) and 247 m × 927 m at 74°N (northern end), totaling 41,502,435 land cells over the continent. Lateral boundary condition of zero head is set at the sea level along the coast. Starting the initial water table at the land surface, we solve the flow equations iteratively until the head stabilizes at all cells (Δh/iteration <1 mm). With parallel processing, a run can be completed in 2 days on 64 processors of the Finis Terrae computer at the Supercomputer Center of Santiago de Compostela, Galicia, Spain (Centro de Supercomputación de Galicia, CESGA). We note that this computation is intended to be performed off-line, not interactive with other components of earth system models. It is also intended to be performed at climate equilibrium time scales, scales relevant to wetland establishment (hydric soil formation, peat accumulation and vegetation succession), such as century to millennium time steps at which fundamental shifts in hydrology occurs.

With lateral, cell to cell, groundwater convergence, river and wetland cells appear in the simulation where the water table rises to the land surface. At these cells, the water table is kept at the land surface, mimicking river and ET removal in nature. The simulation results are shown in Fig. 8d–f corresponding to the three recharge forcings.

4.6 Validation with water table observations

We compiled water table observations at 567,946 sites in the US from the entire USGS archive over 1927–2005 (Fig. 9). A detailed description of the data is given in Fan et al. 2007. About 81% of the sites have one reading taken sometime in the past; that is, each data point has a different time stamp and the map contains some temporal noise. Also, the sites are mostly at low elevations and river valleys, which will introduce a spatial bias in the dataset. In addition, groundwater pumping has lowered the water table over large regions (orange in Fig. 9). But this is the best data available and we will use it to validate model simulations bearing in mind potential problems. Recently we compiled 623 observations from six Canadian provinces and the Canadian wetland database. We evaluate the simulation at 360,889 model cells that contain observations. We examine the statistics of the residual (simulated–observed head), which should follow a Gaussian distribution with a zero mean and no systematic dependence on climate and terrain. The residual statistics are shown in Fig. 10 for the three simulations, and we make the following observations.

(1) The histograms of the residuals are close to Gaussian. In the CLM run, results at 16% of the cells are within 1 m of observations, 43% within 5 m, 65% within 10 m, and 83% within 20 m. Using Mosaic run, they are 16, 41, and 80%, respectively. Using Noah, they

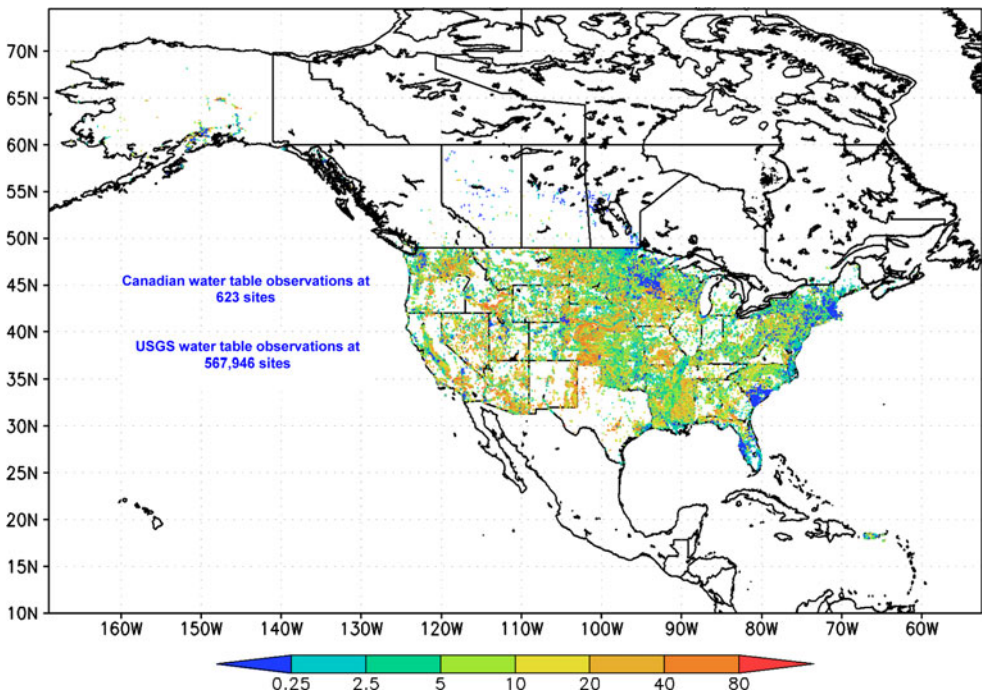

Fig. 9 Observed water table depth (WTD, in m) in N. America

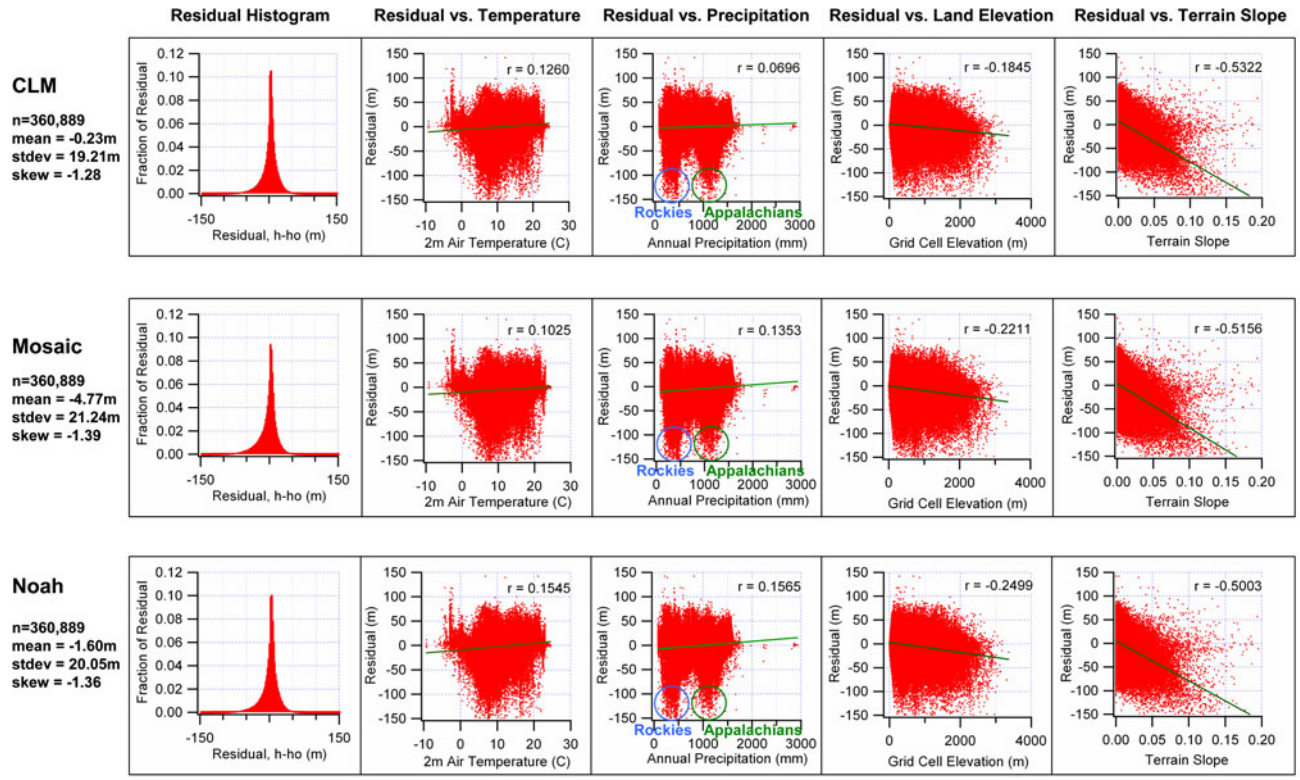

Fig. 10 Validation of the three simulations forced by CLM, Mosaic, and Noah estimated recharge (*top* to *bottom*) against water table observations. From *left* to *right*: histogram of the residual (modeled head–observed head), residual versus temperature, versus annual precipitation, versus grid cell elevation, and versus terrain slope, with the Pearson correlation coefficient r given

are 16, 42, and 82%, respectively. Given the wide range of climate and terrain conditions, the simple parameterization, the uncertainty in recharge forcing, and the noise and bias in the observations, we consider the agreement with observations acceptable.

(2) The mean of the residual is slightly negative for all three simulations (−0.23 m from CLM, −4.77 m from Mosaic, and −1.60 m from Noah) as related to the negative skew (longer tail on the left). To diagnose where the large negative bias occurred, we plot the residual versus key climate and terrain variables. Negative bias occurs at cooler and drier climate and higher and steeper terrain. Two clusters of low bias are visible in the residual versus *P* plot, with the first (circled blue) corresponding to the Rockies at the 200–500 mm *P* range, and the second (green) corresponding to the Appalachians at the 1,000–1,250 mm *P* range (Fig. 6d). There are two likely reasons. First, the model grid spacing (30 sec., >900 m) is too large to resolve the intricate valleys and to compare with point observations in rough terrain. In nature, the high local topographic relief redistributes the available recharge into local valleys, creating locally high water table (as observed by USGS monitoring wells); in the model, the large flat cell only drains to the next flat cell, which, although mimics the regional drainage well, obliterates local drainage. Second, the GLDAS recharge is likely too low in the mountains (near zero) to sustain perennial mountain streams observed in nature. Although a 10 mm minimum recharge is specified in the model, it is insufficient to maintain the observed high water table in the high valleys.

(3) The peak of the histogram occurred not at zero, but at 1.02, 0.98, and 1.01 m, respectively, suggesting a slight high model bias. Residual versus climate and terrain plots suggest that the high bias occurs at warmer and wetter climate (positive correlation with temperature and *P*), and lower and flatter terrain (negative correlation with elevation and slope). It is attributed to widespread groundwater pumping which lowers the observed water table in regions occupying mild climate and low-flat valleys and coastal regions.

It is expected that the low model bias in the mountainous regions (observation 2 above) will affect Type-A wetland estimates (local runoff fed), but the slight high bias in developed regions due to pumping (low bias in observations, three above) will have little effect on wetland delineation.

5 Comparison with Mapped Wetlands

A few broad features are apparent in the simulated water table (Fig. 11a, Noah recharge): shallow water table is found in three types of settings. The first is in a humid climate over flat lowland, e.g., the lower Mississippi valley and the coastal plains. These regions correspond closely to the large wetlands found here (Fig. 3b). The second shallow water table setting is in the boreal region, e.g., the Hudson Bay lowlands, where frozen ground and proximity to sea level are the primary cause. They correspond closely to the large mapped wetlands here (Fig. 3b). The third shallow water table setting is in the arid/semi-arid climate, but with large regional groundwater convergence, such as the inter-mountain valleys of western US where snowmelt in the mountains feeds the aquifers in the valleys, and the arid western Texas Gulf coast and the Baja coast, where groundwater, sourced in interior highlands, emerges before the sea. In these three settings, the shallow water table must be the primary 'wetting mechanism' for the wetlands, giving rise to the broad resemblance between Figs. 3b and 11a. A strong resemblance is also apparent at a more local scale as one compares Fig. 11b with f, c with g (left map), and d with h (left map). A more quantitative comparison is made below by breaking down the continent into first, temperate regions (lower 48 states of the US) and cold regions (Alaska and Canada), and second, within each region, states and provinces, in order to assess the model performance over the wide range of climate and terrain conditions and wetland types.

5.1 Pre-settlement wetlands in the lower 48 states of the US

We compare the location and extent of shallow water table to mapped wetlands in the lower 48 states. Systematic conversion of wetlands for agriculture since European settlement has destroyed 53% of the natural wetlands in the

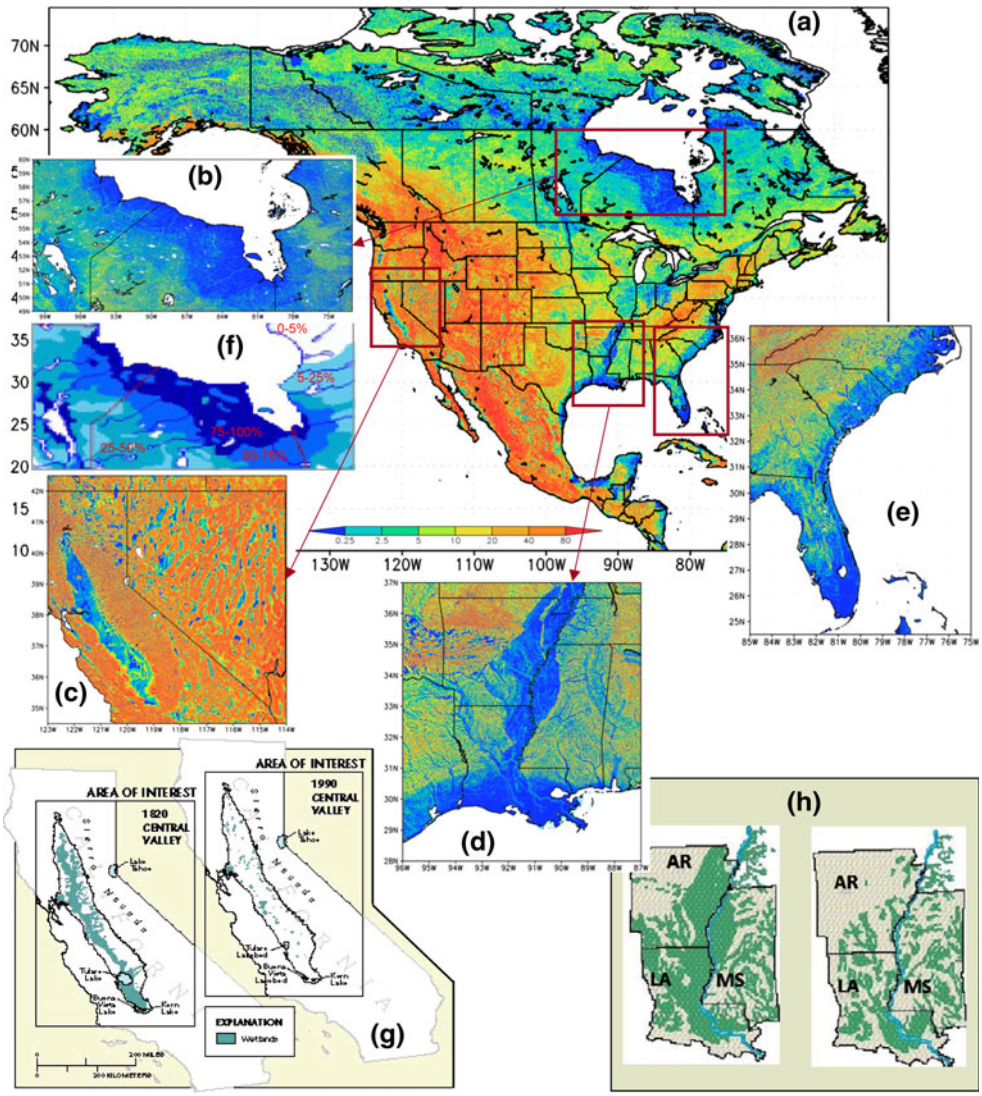

Fig. 11 **a** Simulated equilibrium water table depth with Noah recharge, **b–e** details over four regions of abundant wetlands, **f** mapped wetlands in Hudson Bay lowlands (from Natural Resource Canada), **g** loss of wetlands in California Central Valley (from Dahl and Allord 1997), and **h** loss of bottomland forest swamps in lower Mississippi Valley (from Putnam et al. 1960 and 1982 data from U.S. Fish and Wildlife Service, Vicksburg, Mississippi)

lower 48 states (Dahl 1990). The extent of loss is seen in the California Central Valley (Fig. 11g) and the lower Mississippi valley (Fig. 11h). Because wetland draining practice (ditches, tiles) is difficult to incorporate into the model, the comparison is made with pre-settlement estimates from Dahl 1990. The latter is based on multiple sources including colonial or state records, historic maps of hydric soils, land use conversion records and drainage statistics, and may contain uncertainties due to the lack of quantitative mapping and shifting political boundaries in early settlement times. Yet it is the most complete quantitative reconstruction of natural wetland distribution and extent, and hence it will be used here.

To determine the threshold water table depth for wetland conditions, we resort to wetland water table observations in the literature for guidance of reasonable cutoff depth. We compiled recent data from published literature (see http://envsci.rutgers.edu/~yreinfelder/wetland_water_table_obs.pdf) which suggest a range of 0–1.5 m, with a mean of 0.40 m. The 359 water table depth observations in the Canadian wetland database averaged 0.20 m (http://wetlands.cfl.scf.rncan.gc.ca/norx368/info-eng.asp). We evaluated several thresholds, and a threshold of 0.25 m seems to give reasonable estimates of wetland areas from the simulations. The left column in Fig. 12 plots the area with water table depth <0.25 m versus mapped wetland area in the 48 states for the three simulations. We note the following patterns.

(1) Overall, the simulations successfully capture the continental-scale distribution of wetlands as represented by the 48 states across a wide range of climate and terrain conditions, as suggested by the high correlation coefficients (0.8882, 0.8300, and 0.8772 for CLM, Mosaic, and Noah, respectively). The large wetland area in Texas, mostly arid but with extensive coastal wetlands along the Gulf, is well represented in CLM and Noah runs, a result of regional groundwater convergence from interior highlands before the sea.

(2) All three simulations tend to under-estimate coastal wetlands (green lettering). Mosaic gives the lowest as a result of its unrealistically low recharge over the humid and sandy coastal plains. A synthesis study by the USGS (Delin and Risser 2007), based on multiple field methods, gives a mean of ~600 mm/year in N. Carolina (NC), but Mosaic gives ~80 mm/year, CLM ~180 mm/year and Noah ~260 mm/year (noted on Fig. 8a–c) the latter gives the best wetland estimate among the three. Another USGS field study (Noble 1997) near Houston, Texas, gives 150 mm/year, close to CLM and Noah (Fig. 8a–c) but grossly under-estimated by Mosaic (<25 mm/year) which gives the least wetland in Texas (TX). The results suggest that the simulated wetland depends on the accuracy of recharge; where the recharge is closer to observations, so is the model wetland.

(3) All three simulations consistently under-estimate the wetlands in cold regions (blue lettering). It is at least partially due to the unrealistically low recharge. Over Minnesota (MN), the USGS synthesis (Delin and Risser 2007) reports ~300 mm/year, but CLM gives ~80 mm/year, Mosaic ~30 mm/year, and Noah ~50 mm/year (Fig. 8a–c), with CLM giving the best wetland estimate. Over Wisconsin (WI), the USGS study reports ~300 mm/year, but CLM gives ~150 mm/year, Mosaic ~90 mm/year, and Noah ~110 mm/year (Fig. 8a–c), with CLM giving the best, albeit still low, estimate. This again illustrates the importance of realistic recharge; in both MN and WI cases, the more accurate recharge (CLM) consistently gives more accurate wetland estimates.

(4) All three simulations over-estimate the arid states (orange lettering). The incorrectly high recharge in the arid internal-drainage basins is considered the primary cause. In internal-drainage basins, recharge in the valleys must be negative to balance the high precipitation in the mountains which flows to the valleys. Evaporation from the floor of Pilot Valley near the Nevada-Utah border was estimated to be 1,380 mm/year based on multiple field methods (Lines 1979). Given that precipitation is about 80 mm/year (Fan et al. 1997), the recharge is about −1,300 mm/year. But all three GLDAS recharge estimates are positive (10–40 mm/yr) (Fig. 8a–c). Mosaic has the lowest recharge which gives the best estimate of wetlands in Nevada and Utah, and Noah has the highest recharge which gives the worst estimates. This again illustrates the importance of recharge. A negative recharge cannot be achieved in GLDAS models without lateral groundwater flow from the mountains, pointing to the need to include groundwater flow in the models themselves.

(5) Both CLM and Noah simulations tend to over-estimate wetlands in the humid and hilly Appalachian states (black lettering), unexpected since the simulated water table has a low bias here (Fig. 10). The apparent inconsistency between the two sets of observations (wetland area and water table depth) is a result of rough terrain that cannot be resolved at the 30 sec. grid spacing. Here, a high water table in the narrow valleys (as observed by USGS) only results in small linear wetlands (as mapped by USFWS). A large grid, when elevated to match the observed water table, will inevitably result in large wetlands. The effect of grid spacing is further examined blow (Fig. 13). This is also a partial cause for the over-

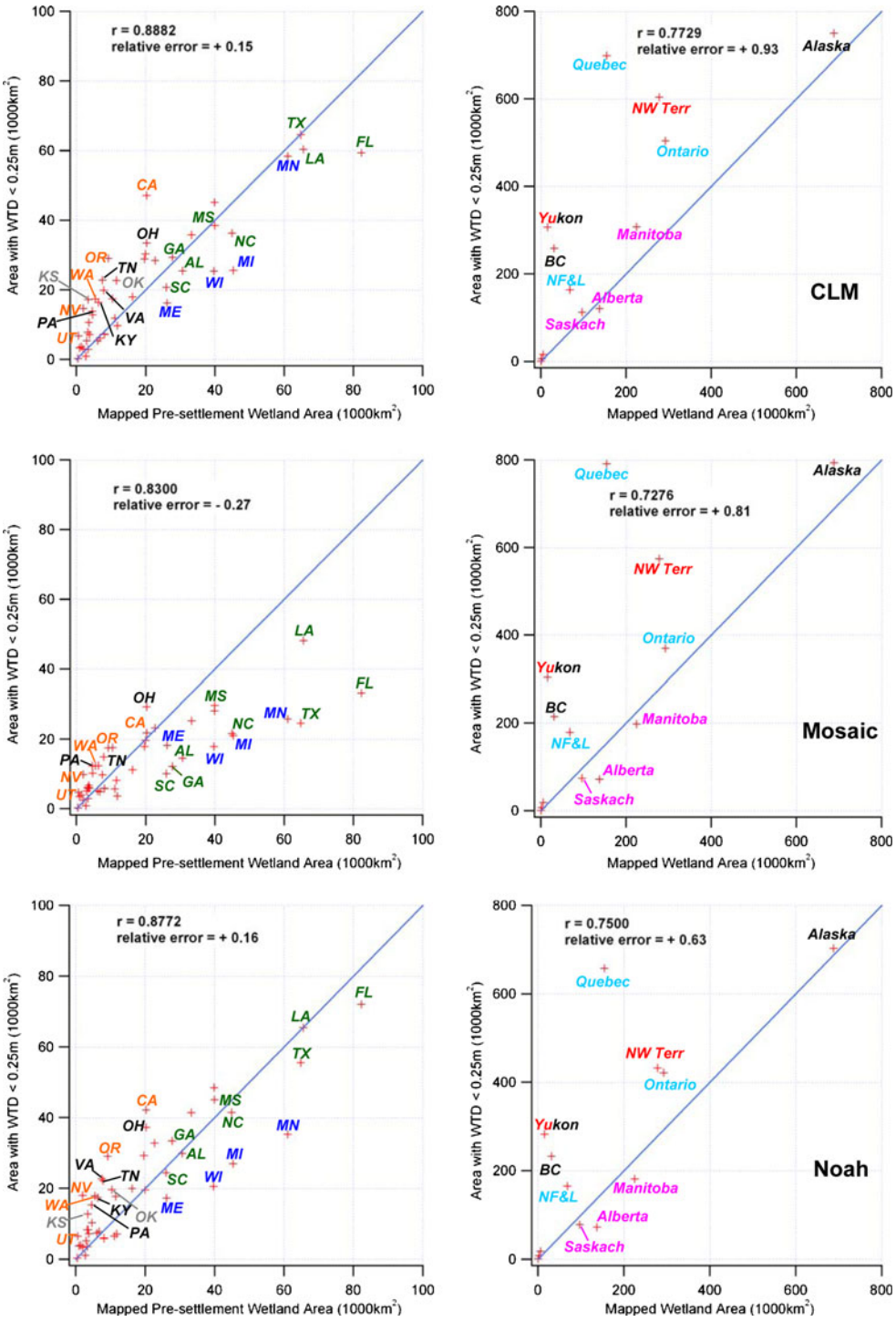

Fig. 12 Area with simulated water table depth <0.25 m versus area of mapped wetlands. *Left* column: lower 48 states, *right* column: Alaska and Canada. Pearson correlation coefficient is given as r

estimates in the mountainous states in the arid and semi-arid west (orange lettering).

(6) Both CLM and Noah forced simulations tend to overestimate wetlands in the US High Plains (grey lettering) characterized by a deep blanket-sand-gravel aquifer (http://capp.water.usgs.gov/gwa/). The great thickness enhances drainage which leads to a lower water table, but this unique sedimentary feature is not captured in the simple model here. Regional-scale geologic features, such as depth to bedrock, are essential information needed to improve the simulation, but they are not yet included in global terrain datasets.

Given the uncertainties in recharge, as manifested by the large difference among the three estimates, and the fact that

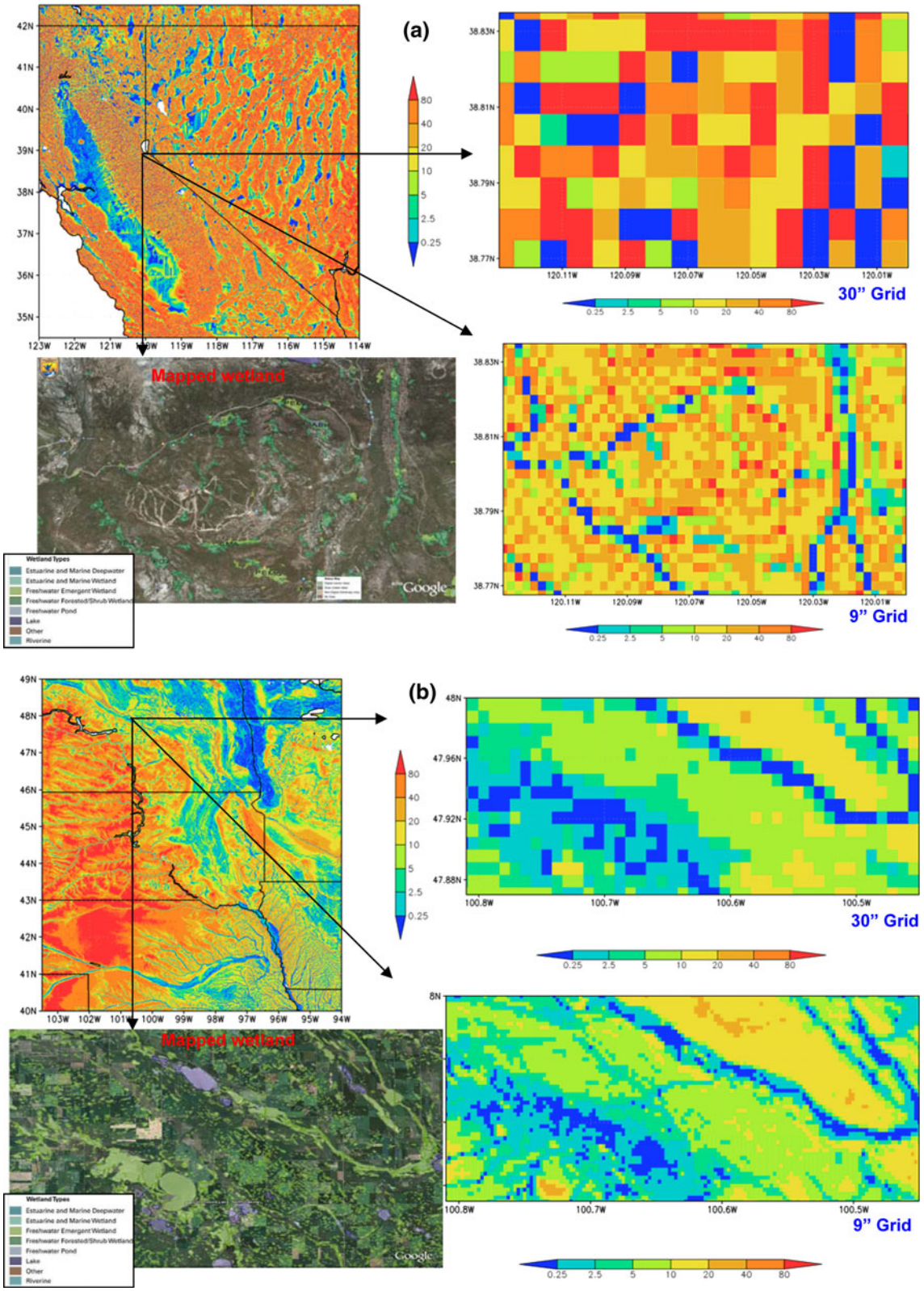

Fig. 13 Effect of model grid (30 sec. vs. 9 sec.) on wetland simulation (blue cells, water table depth <0.25 m) as compared to mapped wetlands, **a** a mountain wetland complex in the Sierra Nevada south of Lake Tahoe, and **b** at the Prairie Potholes near Cottonwood Lakes in N. Dakota

a better recharge indeed results in better wetland estimate, we consider the performance of the model reasonable in the temperate regions of the continent. It broadly captures the continental scale and regional scale features in wetland distribution and extent under a wide range of climate and terrain settings.

5.2 Wetlands in Alaska and Canada

Over 70% of wetlands in N. America are located in Canada and Alaska, primarily influenced by impeded drainage due to seasonal ground frost or permafrost under a thin active layer. Comparison is made separately to evaluate the model performance in this environment (Type-F wetlands). Unfortunately, the digital topography in Canada consists of a patchwork of varying resolution (Fig. 5c) leading to inconsistent terrain slope and water table estimates across the border of the patches. Therefore we give primary weight to Alaska which has the same high-quality topographic and wetland mapping as in the lower 48 states, and the lower Canadian provinces where the coarse topography has been replaced (Fig. 5c).

Wetland area in Alaska is obtained from (Dahl 1990) as the pre-settlement acreage although it has not been significantly affected by humans (1% loss). Wetland areas in Canada are from the Atlas of Canada (http://atlas.gc.ca/sitefrancais/english/learningresources/theme_modules/wetlands/index.html). Figure 12 (right column) gives the comparison between simulated and mapped wetlands. We make the following remarks.

(1) All three simulations grossly over-estimate wetlands in eastern Canada (bright blue lettering, Quebec, Ontario, Newfoundland and Labrador or NF&L). We contribute this to the gross over-estimate of recharge by the three GLADS models. A water balance study in southern Quebec (Nastev et al. 2006) reports a recharge of ~58 mm/year, while CLM gives 200–300 mm/year, Mosaic 300–400 mm/year, and Noah 200–300 mm/year (Fig. 8a–c), with Mosaic giving the highest bias. A similar study in southern Ontario (Meriano and Eyles 2003) reports a recharge of 110 mm/year, while all three models give 200–300 mm/year (Fig. 8a–c). These very high recharge rates had large effects on the water table in this flat and low region.

(2) The large over-estimate in Northwest Territory and Yukon (red lettering) in all three simulations is largely caused by the coarse digital topography (red region in Figs. 5c, 2-4 times coarser than blue). The resulting flatter slope lead to slower drainage and higher water table, giving large wetland areas north of 60°N (Fig. 11a). The effect is further exacerbated in Yukon due to high natural relief. It also contributed to the positive bias in Quebec which has a portion north of 60°N.

(3) All three simulations over-estimate wetlands in the mountain chains in the west (Alaska, Yukon, and British Columbia or BC) (black lettering), which we attribute to the coarse grid over rough terrain as discussed earlier and further examined later (Fig. 13).

(4) Both Mosaic and Noah slightly under-estimate wetlands in the Prairie Provinces (magenta lettering). The primary reason is the grid resolution (30 sec., ~900 m) which is too coarse to resolve the individual potholes or sloughs which are 30–200 m across (Zhang and Allen 2004), as shown later (Fig. 13). It may also be a partial cause for under-estimation in the Prairie states of the US (the Dakotas and Minnesota).

Overall, wetlands in Canada are grossly over-estimated due to the unlikely high recharge in eastern Canada and the coarse terrain grid in northern Canada. The high correlation coefficient between simulated and mapped wetlands illustrates the value of the water table as a first-order indicator of wetland conditions. We note that the qualities of forcing and terrain data are not inherent deficiencies of the framework. With improved land hydrologic modeling and with improved global terrain data in the future, the advantage of the water table as a wetland indicator will likely to be more apparent.

In the above discussions, the over-estimate in mountain wetlands and the under-estimate in Prairie pothole wetlands were attributed to the coarse grid resolution in the model. Figure 13 illustrates the effect of grid size by comparing simulations at 30 sec. (~925 m) and 9 sec. (~275 m). At a location in the Sierra Nevada mountains (Fig. 13a), mapped wetlands (http://www.fws.gov/wetlands/Data/GoogleEarth.html) are linear features in the narrow valleys, which are well simulated by the 9 sec. grid (blue cells, water table depth <0.25 m) but poorly represented by the 30 sec. grid as large, broken patches. The wetland area in the 30 sec. grid is 2.8 times of the area in the 9 sec. grid. At a location in the Prairie potholes near Cottonwood Lakes in N. Dakota (Fig. 13b), where the USGS has conducted numerous field studies (e.g., Winter and Rosenberry 1995), the mapped wetlands take three forms: large patches (lower left), linear bands (upper right), and numerous isolated small patches (potholes, throughout the map). The 30 sec. grid captured the large patches and exaggerated the large linear band for the same reasons as in Fig. 13a, but it missed all the small, isolated potholes. The 9 sec. grid captured both the large patches and the linear bands well, but it missed almost all of the small, isolated potholes. Even at 9 sec. (~275 m), the individual potholes (30–200 m across) cannot be resolved. Unless the grid resolution is smaller

than the potholes, wetland in this environment will not be fully captured by this method.

Finally, we note the close agreement between the mapped wetlands and the simulated wetlands at the 9 sec. grid. It illustrates the importance of cell-to-cell groundwater convergence at smaller scales. Lateral redistribution is important to representing continental-scale wetlands due to large-scale convergence and the sea level boundary condition. Lateral redistribution is equally and perhaps more important to representing small wetlands due to local convergence because the topographic relief is more pronounced at such scales. The limitation lies in the grid size.

6 Summary and discussions

The objectives of the study were to, first, provide a synthesis of key hydrologic mechanisms of wetland formation, and second, formulate and test a simple framework for simulating wetlands in global climate and earth system models. Below we summarize our efforts and findings.

(1) The synthesis suggests that natural wetlands can be classified into four end-member types, Type-A: mostly precipitation and local surface/subsurface runoff-fed, Type-D: mostly surface water-fed but groundwater-supported, Type-E: mostly groundwater-fed, and Type-F: mostly frozen ground-supported. Wetlands can be found along a continuum defined by these end-members and may have contributions from more than one mechanism, but these end-members need to be represented simultaneously in a modeling framework in order to capture the wide range of wetlands encountered at continental and global scales.

(2) The synthesis underscores the role of the groundwater in sustaining large and stable wetlands. It supports surface water-fed wetlands by maintaining a saturated substrate, directly feeds wetlands, and constrains land drainage by the sea level. It also regulates CH_4 flux from wetlands. Because lateral groundwater flow and the water table position are not yet included in climate and earth system models, a key mechanism of wetland formation has been left out.

(3) We developed a simple framework for wetland simulation using the water table depth as a first order indicator of wetland conditions. The water table position reflects the long-term balance between the climate input and the terrain-induced and sea level constrained drainage. Constructing the equilibrium water table requires climate forcing as water table recharge, obtained as $R = P - \mathrm{ET} -$ surface runoff. It also requires terrain slope and winter temperature to parameterize soil depths, and the sea level as the boundary condition of known water table heads. To address the sensitivity of the method to forcing uncertainties, we performed the simulation using model estimates from three GLDAS land models.

(4) Comparison against mapped wetlands suggests that the method can capture the most prominent continental-scale features in wetland distribution and extent, particularly large valley and coastal wetlands formed by large-scale groundwater convergence, and the boreal and sub-arctic wetlands caused by poor drainage over frozen grounds. This is a direct result of lateral groundwater divergence/convergence among the model cells, a key process for the formation and maintenance of large and stable wetlands, but absent in current wetland modeling approaches. A wetland simulation scheme based on soil moisture and land slope, as commonly adopted, will have difficulties finding wetlands along the Atlantic and Gulf coast; the sandy coastal plain soils will drain the rainfall quickly, and without the shallow water table, the drainage is allowed to occur below sea level, causing soil moisture to be near the wilting point (Miguez-Macho et al. 2008) which cannot be interpreted as wetlands, although extensive wetlands are found here.

(5) Comparison between simulations at different grid resolutions suggests that at finer grids, the framework may be equally capable of simulating small wetlands perched in high valleys or isolated as potholes. Cell-to-cell groundwater flow is arguably more important at hillslope scales in redistributing moisture surplus or deficit in regions of high local relief. Sub-grid characterization, as commonly applied in global models, will provide a solution if the interests are to represent these small wetlands.

(6) Our study shows that the accuracy of the simulated wetlands depends on that of recharge forcing. Where the recharge is closer to independent field observations, so is the estimated wetland. Given the fact that a globally consistent recharge estimate must be obtained from model simulations and that these models do not yet include the groundwater processes that affect recharge, such estimates will remain conceptually and quantitatively flawed. A meaningful approach would be to explicitly include the groundwater processes in these models. An important objective for the community is to reconstruct global wetlands in the past and the future in response to changes in climate, ice extent and sea level. Given the importance of the groundwater, the objective would be best achieved if the models explicitly track the groundwater mass balance. Its role in controlling continental-scale soil moisture, ET, P, river flow, and river basin water budget has been investigated by

several recent studies (e.g., Liang et al. 2003; Yeh and Eltahir 2005; Yu et al. 2006; Niu et al. 2007; Maxwell et al. 2007; Fan et al. 2007; Miguez-Macho et al. 2007, 2008; Anyah et al. 2008; Schaller and Fan 2009, among others), which suggest that the groundwater reservoir is an integral part of the terrestrial water cycle. Its role in global wetland water-carbon dynamics needs to be similarly examined through dynamically coupled model simulations. In the absence of that, the framework presented here may provide an alternative approach.

Acknowledgments This work is supported by the US National Science Foundation, Ramón y Cajal program of the Spanish Ministry of Education and Science, Rutgers University Academic Excellence Fund, and the supercomputer center (Centro de Supercomputación de Galicia, CESGA) at Santiago de Compostela, Galicia, Spain. We thank the following colleagues for assisting us in obtaining water table observations from provincial government archives: In Canada, Azina Kanji and Carole Holt Oduro at Alberta Environment; Kei Lo at Saskatchewan Watershed Authority; Bob Betcher and Janie Ulrich at the Manitoba Water Stewardship; Dajana Grgic and Christina Girjoaba at the Ontario Ministry of the Environment; Fern Schultz, Celine Davis, and Lindsey MacFarlane at British Columbia Ministry of the Environment; In the US, the scientists and staff at the US Geological Survey for nearly a century of systematic monitoring of the nation's water resources and for maintaining a state-of-art national database. The above individuals answered numerous emails from us and have gone out of their ways to assemble the complete observations for us (location, well depth, aquifer type, well history, human influence, and water table time series). The efforts of those individuals who have collected data in the fields over decades made the work possible. Finally, we express our sincere thanks to the editor and anonymous reviewers who have raised constructive criticisms which significantly improved the manuscript.

References

Ahnert F (1970) Functional relationships between denudation, relief, and uplift in large mid-latitude drainage basins. Am J Sci 268:243–263

Anyah R, Weaver CP, Miguez-Macho G, Fan Y, Robock A (2008) Incorporating water table dynamics in climate modeling: 3. Simulated groundwater influence on coupled land-atmosphere variability. J Geophys Res. doi:10.1029/2007JD009087

Ashley GM, Goman M, Hover VC, Owen RB, Renaut RW, Muasya AM (2002) Artesian blister wetlands, a perennial water resource in the semi-arid rift valley of East Africa. Wetlands 22(4):686–695

Bao R, Alonso A, Delgado C, Pages JL (2007) Identification of the main driving mechanisms in the evolution of a small coastal wetland (Traba, Galicia, NW Spain) since its origin 5700 cal yr BP. Palaeogeogr Palaeoclimatol Palaeoecol 247(3–4):296–312

Barbiero L, Netol JPD, Ciornei G, Sakamoto AY, Capellari B, Fernandes E, Valles V (2002) Geochemistry of water and groundwater in the Nhecolandia, Pantanal of Mato Grosso, Brazil: variability and associated processes. Wetlands 22(3):528–540

Bastl M, Burian M, Kucera J, Prach K, Rektoris L, Stech M (2008) Central European pine bogs change along an altitudinal gradient. Preslia 80:349–363

Beven KJ, Kirkby MJ (1979) A physically based, variable contributing area model of basin hydrology. Hydrol Sci Bull 24:43–69

Boenzi F, Caldara M, Pennetta L, Simone M (2006) Environmental aspects related to the physical evolution of some wetlands along the Adriatic coast of Apulia (Southern Italy): a review. J Coastal Res 1(Sp. Iss. 39):170–175

Bosman AF, van der Molen PC, Young R, Cleef AM (1993) Ecology of a Paramo cushion mire. J Veg Sci 4:633–640

Bowler JM (1986) Spatial variability and hydrologic evolution of Australian lake basins: analogue for Pleistocene hydrologic change and evaporate formation. Palaeogeogr Palaeoclimatol Palaeoecol 54:21–41

Brandy NC (1984) The nature and properties of soils, 9th edn. Macmillan, New York, p 750

Brook EJ, Harder S, Severinghaus J, Steig EJ, Sucher M (2000) On the origin and timing of rapid changes in atmospheric methane during the last glacial period. Global Biogeochem Cycles 14:559–572

Carrington DP, Gallimore RG, Kutzbach JE (2001) Climate sensitivity to wetlands and wetland vegetation in mid-Holocene North America. Clim Dyn 17:151–157

Chapman JB, Lewis B, Litus G (2003) Chemical and isotopic evaluation of water sources to the fens of South Park, Colorado. Env Geol 43:533–545

Chappellaz JA, Fung IY, Thompson AM (1993) The atmospheric CH_4 increase since the Last Glacial Maximum (1) source estimates. Tellus B 45(3):228–241

Chen J, Kumar P (2001) Topographic influence on the seasonal and interannual variation of water and energy balance of basins in North America. J Clim 14:1989–2014

Clapp RB, Hornberger GM (1978) Empirical equations for some soil hydraulic properties. Water Resour Res 14:601–604

Cole CA, Brooks RP, Wardrop DH (1997) Wetland hydrology as a function of hydro-geomorphic (HGM) subclass. Wetlands 17(4):456–467

Cowardin LM, Carter V, Golet F, LaRoe ET (1979) Classification of wetlands and deepwater habitats of the United States, US Department of the Interior, Fish and Wildlife Service (http://www.fws.gov/nwi/Pubs_Reports/Class_Manual/class_titlepg.htm)

Dahl TE (1990) Wetlands losses in the United States 1780'S to 1980'S. US Department of the Interior, Fish and Wildlife Service, Washington, p 13

Dahl TE, Allord GJ (1997) History of wetlands in the conterminous United States, USGS Water-Supply Paper 2425 (http://water.usgs.gov/nwsum/WSP2425/)

Dallenbach A, Brunier T, Fluckiger J, Stauffer B, Chappellaz J, Raynaud D (2000) Changes in the atmospheric CH_4 gradient between Greenland and Antarctica during the last glacial and transition to Holocene. Geophys Res Lett 27:1005–1008

Davidson EA, Keller M, Erikson HE, Verchot LV, Veldkamo E (2000) Testing a conceptual model of soil emissions of nitrous and nitric oxide. Bioscience 50:667–680

Decharme B, Douville H, Prigent C, Papa F, Aires F (2008) A new river flooding scheme for global climate applications: off-line evaluation over South America, J Geophy Res. doi:10.1029/2007JD009376

Delin N, Risser DW (2007) Groundwater recharge in humid areas of the United States—a summary of Groundwater Resources Program studies, 2003–2006, USGS Fact Sheets FS-2007-3007

Deming D (2002) Introduction to hydrogeology. McGraw-Hill, New York, p 468

Dendy FE, Bolton GC (1976) Sediment yield-runoff-drainage area relationships in the United States. J Soil Water Conserv 32:264–266

Ducharne A, Koster RD, Suarez MJ, Stieglitz M, Kumar P (2000) A catchment-based approach to modeling land surface processes in a general circulation model: 2. Parameter estimation and model demonstration. J Geophys Res 105:24823–24838

Duffy CJ, Al-Hassan S (1988) Groundwater circulation in a closed desert basin: topographic scaling and climatic forcing. Water Resour Res 24(10):1675–1688

Dunn AL, Barford CC, Wofsy SC, Goulden ML, Daube BC (2007) A long-term record of carbon exchange in a boreal black spruce forest: means, responses to interannual variability, and decadal trends. Glob Chang Biol 13(3):577–590

Dwire KA, Kauffman JB, Baham JE (2006) Plant species distribution in relation to water table depth and soil redox potential in Montane riparian meadows. Wetlands 26(1):131–146

Euliss NH Jr, LaBaugh JW, Fredrickson LH, Mushet DM, Laubhan MK, Swanson GA, Winter TC, Rosenberry DO, Nelson RD (2004) The wetland continuum: a conceptual framework for interpreting biological studies. Wetlands 24(2):448–458

Fan Y, Duffy CJ, Oliver DS Jr (1997) Density-driven groundwater flow in closed desert basins: field investigations and numerical experiments. J Hydrol 196:139–184

Fan Y, Miguez-Macho G, Weaver CP, Walko R, Robock A (2007) Incorporating water table dynamics in climate modeling: 1. Water table observations and equilibrium water table simulations, J Geophys Res. doi:10.1029/2006JD008111

Faure HF, Walter RC, Grant DR (2002) The coastal oasis: ice age springs on emerged continental shelves. Glob Planet Change 33:47–56

Freeze RA, Cherry JA (1979) Groundwater. Prentice-Hall, New Jersey, p 604

Funk DW, Pullman ER, Peterson KM, Crill PM, Billings WD (1994) Influence of water-table on carbon- dioxide, carbon-monoxide, and methane fluxes from Taiga bog microcosms. Global Biogeochem Cycles 8(3):271–278

Gaiser EE, Taylor BE, Brooks MJ (2001) Establishment of wetlands on the southeastern Atlantic coastal plain: paleolimnological evidence of a mid-Holocene hydrologic threshold from a South Carolina pond. J Paleolimnol 26:373–391

Gedney N, Cox PM (2003) The sensitivity of global climate model simulations to the representation of soil moisture heterogeneity. J Hydrometeorol 4:1265–1275

Gedney N, Cox PM (2004) Climate feedback from wetland methane emissions. Geophys Res Lett 31:L20503. doi:10.1029/2004GL020919

Girard P, da Silva CJ, Abdo M (2003) River-groundwater interactions in the Brazilian Pantanal: the case of the Cuiaba River. J Hydrol 283(1–4):57–66

Gosselin DC, Drda S, Harvey FE, Geoeke L (1999) Hydrologic setting of two interdunal valleys if the central Sand Hills of Nebraska. Ground Water 37(6):924–933

Grevilliot F, Krebs L, Muller S (1998) Comparative importance and interference of hydrologic conditions and soil nutrient gradients in floristic biodiversity in flood meadows. Biodivers Conserv 7(11):1495–1520

Groom PK (2004) Rooting depth and plant water relations explain species distribution patterns within a sandplain landscape. Funct Plant Biol 31(5):423–428

Gutentag ED, Heimes FJ, Krothe NC, Lucekey RR, Weeks JB (1984) Geohydrology of the High Plains aquifer in parts of Colorado, Kansas, Nebraska, New Mexico, Oklahoma, South Dakota, Texas, and Wyoming, USGS Professional Paper 1400-B

Hajkova P, Hajek M, Apostolova I (2006) Diversity of wetland vegetation in the Bulgarian high mountains, main gradients and context dependence of the pH role. Plant Ecol 184:111–130

Harris RC, Sebacher DI, Day FP Jr (1982) Methane flux in the Great Dismal Swamp. Nature 297:673–674

Hayashi M, Rosenberry DO (2002) Effects of groundwater exchange on the hydrology and ecology of surface waters. Ground Water 40:309–316

Hooke RB (2000) Toward a uniform theory of clastic sediment yield in fluvial systems. Geol Soc Am Bull 112:1778–1786

Hunt RJ, Walker JF, Krabbenhoft DP (1999) Characterizing hydrology and the importance of ground-water discharge in natural and constructed wetlands. Wetlands 19(2):458–472

Ju WM, Chen JM, Black TA, Barr AG, McCaughey H, Roulet NT (2006) Hydrologic effects on carbon cycles of Canada's forests and wetlands. Tellus B 58(1):16–30

Jungkunst HF, Fiedler S (2007) Latitudinal differentiated water table control of carbon dioxide, methane and nitrous oxide fluxes from hydromorphic soils: feedbacks to climate change. Glob Chang Biol 13:2668–2683

Jungkunst HF, Fless H, Scherber C, Fiedler S (2008) Groundwater level controls CO_2, N_2O and CH_4 fluxes of three different hydromorphic soil types of a temperate forest ecosystem. Soil Biol Biochem 40:2047–2054

Kaplan JO (2002) Wetlands at the last glacial maximum: distribution and methane emissions, Geophys Res Lett. doi:10.1029/2001GL013366

Koster RD, Suarez MJ, Ducharne A, Stieglitz M, Kumar P (2000) A catchment-based approach to modeling land surface processes in a general circulation model: 1. Model structure. J Geophys Res 105:24809–24822

Lafleur PM (2008) Connecting atmosphere and wetland: energy and water vapour exchange. Geography Compass 2/4:1027–1057. doi:10.1111/j.1749-8198.2007.00132.x

Langbein WB, Schumm SA (1958) Yield of sediment in relation to mean annual precipitation. AGU Trans 39:1076–1084

Lehner B, Doll P (2004) Development and validation of a global database of lakes, reservoirs, and wetlands. J Hydrol 196:1–22

Liang X, Xie Z, Huang M (2003) A new parameterization for surface and ground water interactions and its impact on water budgets with the variable infiltration capacity (VIC) landsurface model, J Geophys Res. doi:10.1029/2002JD003090

Lines GC (1979) Hydrology and surface morphology of the Bonneville salt flats and Pilot Valley playa, Utah, USGS Water Supply Paper 2057

Loulergue L, Schilt A, Spahni R, Masson-Delmotte V, Blunier T, Lemieux B, Barnola JM, Raynaud D, Stocker TF, Chappellaz J (2008) Orbital and millennial-scale features of atmospheric CH_4 over the past 800,000 years. Nature 453(7193):383–386

MacDonald GM (2002) The boreal forest. In: Orme AR (ed) The physical geography of North America. Oxford University Press, New York, pp 270–290

Mandernack KW, Lynch L, Krouse HR, Morgan MD (2000) Sulfur cycling in wetland peat of the New Jersey Pinelands and its effect of stream water chemistry. Geochim Cosmochim Acta 64(23):3946–3949

Marra MJ, Alloway BV, Newnham RM (2006) Paleoenvironmental reconstruction of a well-preserved Stage 7 forest sequence catastrophically buried by basaltic eruptive deposits, northern New Zealand. Quaternary Science Reviews 25(17–18):2143–2161

Marshall SJ, Clarke GKC (1999) Modeling North American freshwater runoff through the last glacial cycle. Quat Res 52:300–315

Maxwell RM, Chow FK, Kollet SL (2007) The groundwater-land-surface-atmosphere connection: soil moisture effects on the atmospheric boundary layer in fully-coupled simulations. Adv Water Resour 30(12):2447–2466

Meriano M, Eyles N (2003) Groundwater flow through Pleistocene glacial deposits in the rapidly urbanizing Rouge River–Highland

Creek watershed, City of Scarborough, southern Ontario, Canada. Hydrogeol J 11:288–303
Merot Ph, Squividant H, Aurousseau P, Hefting M, Burt T, Maitre V, Kruk M, Butturini A, Thenail C, Viaud V (2003) Testing a climato-topographic index for predicting wetlands distribution along an European climate gradient. Ecol Modell 163:51–71
Miguez-Macho G, Fan Y, Weaver CP, Walko R, Robock A (2007) Incorporating water table dynamics in climate modeling: 2. Formulation, validation, and soil moisture simulation, J Geophys Res. doi:10.1029/2006JD008112
Miguez-Macho G, Li H, Fan Y (2008) Simulated water table and soil moisture climatology over North America. Bull Am Meteorol Soc 5:663–672
Miola A, Bondesan A, Corain L, Favaretto S, Mozzi P, Piovan S, Sostizzo I (2006) Wetlands in the Venetian Po Plain (northeastern Italy) during the last glacial maximum: interplay between vegetation, hydrology and sedimentary environment. Rev Palaeobot Palynol 141(1–2):53–81
Mitsch WJ, Gosselink JG (2007) Wetlands, 4th edn. John Wiley and Sons, Inc., Hoboken, p 582
Moore TR (1994) Trace gas emissions from Canadian peatlands and the effect of climate change. Wetlands 14(3):223–228
Moore TR, Knowles R (1989) The influence of water table levels on methane and carbon dioxide emissions from peatland soils. Can J Soil Sci 69:33–38
Moore TR, Roulet N, Knowles R (1990) Spatial and temporal variations and methane flux from subarctic- northern boreal fens. Global Biogeochem Cycles 4:29–46
Nastev M, Lefebvre R, Rivera A, Martel R (2006) Quantitative assessment of regional rock aquifers, south- western Quebec, Canada. Water Resour Manage 20:1–18
Nelson FE, Hinkel KM (2002) The far north: a geographic perspective on permafrost environment. In: Orme AR (ed) The physical geography of North America. Oxford University Press, New York, pp 249–269
Niu GY, Yang ZL, Dickinson RE, Gulden LE, Su H (2007) Development of a simple groundwater model for use in climate models and evaluation with GRACE data. J Geophys Res. doi:10.1029/2006JD007522
Noble J (1997) Estimated rate of recharge in outcrops of the Chicot and Evengeline Aquifers near Houston, Texas, USGS Fact Sheets FS-179-97
Owen RB, Renaut RW, Hover VC, Ashley GM, Muasya AM (2004) Swamps, springs and diatoms: wetlands of the semi-arid Bogoria-Baringo Rift, Kenya. Hydrobiologia 518:59–78
Patten DT, Rouse L, Stromberg J (2008) Isolated spring wetlands in the Great Basin and Mojave Deserts, USA: potential response of vegetation to groundwater withdrawal. Environ Manage 41:398–413
Price JS, Branfireun BA, Waddington JM, Devito KJ (2005) Advances in Canadian wetland hydrology, 1999–2003. Hydrol Process 19:201–214
Putnam JA, Furnival GM, McKnight JS (1960) Management and inventory of southern hardwoods, Agricultural handbook, vol 181. US Department of Agriculture, Washington, DC
Raid GK, Wood RD (1976) Ecology of inland waters and estuaries. D. Van Nostrand and Co., New York, p 485
Ramcharan EK (2004) Mid-to-late Holocene sea level influence on coastal wetland development in Trinidad. Quat Int 120:145–151
Rodell M, Houser PR, Jambor U, Gottschalck J, Mitchell K, Meng CJ, Arsenault K, Cosgrove B, Radakovich J, Bosilovich M, Entin JK, Walker JP, Lohmann D, Toll D (2004) The global land data assimilation system. Bull Am Meteorol Soc 85:381–394. http://ldas.gsfc.nasa.gov/GLDAS/docs/obtaindata.shtml)
Rosenberry DC, Winter TC (1997) Dynamics of water-table fluctuations in an upland between two prairie- pothole wetlands in North Dakota. J Hydrol 191:266–289
Rossell IM, Moorhead KK, Alvarado H, Warren RJ (2009) Succession of a southern Appalachian mountain wetland six years following hydrologic and microtopographic restoration. Restor Ecol 17:205–214
Schaller M, Fan Y (2009) River basins as groundwater exporters and importers: implications to water cycle and climate modeling. J Geophys Res. doi:10.1029/2008JD010636
Seuffert G, Gross P, Simmer C, Wood EF (2002) The influence of hydrologic modeling on the predicted local weather: two-way coupling of a mesoscale weather prediction model and a land surface hydrologic model. J Hydrometeorol 3:505–523
Smith LC, MacDonald GM, Velichko AA, Beilman DW, Borisova OK, Frey KE, Kremenetski KV, Sheng Y (2004) Siberian peatlands as net carbon sink and global methane source since the early Holocene. Science 303:353–356
Snyder CT (1962) A hydrologic classification of valleys in the Great Basin, Western United States, In: Neal JT (ed) Playas and dried lakes: occurrence and development, vol 20. Benchmark Papers in Geology, pp. 113–119
Sowers T (2006) Late quaternary atmospheric CH_4 isotope record suggests marine clathrates are stable. Science 311(5762):838–840
Squeo FA, Aravena R, Aguirre E, Pollastri A, Jorquera CB, Ehleringer JR (2006) Groundwater dynamics in a coastal aquifer in north-central Chile: implications for groundwater recharge in an arid ecosystem. J Arid Environ 67:240–254
Stromberg JC, Beauchamp VB, Dixon MD, Lite SJ, Paradzick C (2007) Influence of low-flow and high-flow characteristics to restoration of riparian vegetation along rivers in south-western United States. Freshw Biol 52(4):651–679
Summerfield MA, Hulton NJ (1994) Natural controls of fluvial denudation rates in major world drainage basins. J Geophys Res 99:13871–13883
Thompson Y, Sandefur BC, Miller JO, Karathanasis AD (2007) Hydrologic and edaphic characteristics of three mountain wetlands in southeastern Kentucky, USA. Wetlands 27(1):174–188
U.S. Department of Agriculture (1941) Climates of the United States (46 Maps). http://naldr.nal.usda.gov/NALWeb/Agricola_Link.asp?Accession=yoa1941041
Valdes PJ, Beerling DJ, Johnson CE (2005) The ice age methane budget. Geophys Res Lett. doi:10.1029/2004GL021004
Walko RL, Band LE, Baron J, Kittel TGF, Lammers R, Lee TJ, Ojima D, Pielke RA, Taylor C, Tague C, Tremback CJ, Vidale PL (2000) Coupled atmosphere-biophysics-hydrology models for environmental modeling. J Appl Meteorol 39:931–944
Waller MP, Long AJ, Long D, Innes JB (1999) Patterns and processes in the development of coastal mire vegetation: multi-site investigations from Walland Marsh, Southeast England. Quat Sci Rev 18(12):1419–1444
Walling DE, Webb BW (1983) Patterns of sediment yield. In: Gregory KJ (ed) Background to palaeo-hydrology. Wiley, New York, pp 69–100
Walter BP, Heimann M (2000) A process-based, climate-sensitive model to derive methane emissions from natural wetlands: application to five wetland sites, sensitivity to model parameters and climate. Global Biogeochem Cycles 14(3):745–765
Walter BP, Heimann M, Matthews E (2001a) Modeling modern methane emissions from natural wetlands 1. Model description and results. J Geophys Res 106(D24):34189–34206
Walter BP, Heimann M, Matthews E (2001b) Modeling modern methane emissions from natural wetlands 2. Interannual variations 1982–1993. J Geophys Res 106(D24):34207–34219

Whalen SC (2005) Biogeochemistry of methane exchange between natural wetlands and the atmosphere. Environ Eng Sci 22(1):73–94

Windsor J, Moore TR, Roulet NT (1992) Episodic fluxes of methane from subarctic fens. Can J Soil Sci 72:441–452

Winter TC (1976) Numerical simulation analysis of interaction of lakes and groundwater, USGS Professional Paper 1001, pp 45

Winter TC (1986) Effect of groundwater recharge on configurations of the water table beneath sand dunes and on seepage in lakes in the sandhills of Nebraska. J Hydrol 86:221–237

Winter TC, LaBaugh JW (2003) Hydrologic considerations in defining isolated wetlands. Wetlands 23(3):532–540

Winter TC, Rosenberry DO (1995) The interaction of groundwater with prairie pothole wetlands in the Cottonwood Lake area, east-central North Dakota, 1979–1990. Wetlands 15:193–211

Winter TC, Harvey JW, Franke OL, Alley WA (1998) Ground water and surface water: a single resource. USGS Circular 1139. US Government Printing Office, Denver, p 79

Winter TC, Rosenberry DO, Buso DC, Merk DA (2001) Water source to four US wetlands: implications for Wetland management. Wetlands 21(4):462–473

Winter TC, Rosenberry DO, Kelly E, LaBaugh JW (2005) Comparison of wetlands in different hydrogeologic settings under conditions of extreme climate variability. In: Heathwaite L, Webb B, Rosenberry DO, Weaver D, Hayashi M (eds) Dynamics and biogeochemistry of river corridors and wetlands, vol 294. International Association of Hydrological Sciences Publication, pp 139–147

Woo MK (2002) Wetlands: a hydrological perspective. In: Orme AR (ed) The physical geography of North America. Oxford University Press, New York, pp 146–177

Woo MK, Rowsell RD, Clark RG (1993) Hydrological classification of Canadian prairie wetlands and prediction of wetland inundation in response to climatic variability, Canadian Wildlife Service Occasional Paper No. 79, 24 pp

Yang ZL, Niu GY (2003) The versatile integrator of surface and atmosphere processes—part 1: model description. Global Planet Change 38:175–189

Yeh PJF, Eltahir EAB (2005) Representation of water table dynamics in a landsurface scheme, part I: model development. J Clim 18:1861–1880

Yu Z, Pollard D, Cheng L (2006) On continental-scale hydrologic simulations with a coupled hydrologic model. J Hydrol 331:110–124

Zhang B, Allen G (2004) Landsat analysis of temporal and spatial changes in Prairie Pothole Lakes of North and South Dakota. Geol Soc Am Abstr Prog 36(5):385